



**STUDYING THE EFFECT OF COLD PLASMA ON
THE ETCHING PROCESS OF THE NUCLEAR
TRACK DETECTOR CR-39.**

**2024
MASTER THESIS
DEPARTMENT OF PHYSICS**

Mohammed Khairi Hussein HUSSEIN

**Thesis Advisor
Assist. Prof. Dr. Ferhat BOZDUMAN**

**STUDYING THE EFFECT OF COLD PLASMA ON THE ETCHING
PROCESS OF THE NUCLEAR TRACK DETECTOR CR-39.**

Mohammed Khairi Hussem HUSSEIN

**Thesis Advisor
Assist. Prof. Dr. Ferhat BOZDUMAN**

**T.C.
Karabuk University
Institute of Graduate Programs
Department of Physics
Prepared as
Master Thesis**

**KARABÜK
June 2024**

I certify that in my opinion the thesis submitted by Mohammed Khairi Hussein HUSSEIN. titled “STUDYING THE EFFECT OF COLD PLASMA ON THE ETCHING PROCESS OF THE NUCLEAR TRACK DETECTOR CR-39. ” is fully adequate in scope and in quality as a thesis for the degree of Master of Science.

Assist. Prof. Dr. Ferhat BOZDUMAN

Thesis Advisor, Department Natural and Applied Sciences

This thesis is accepted by the examining committee with a unanimous vote in the Department of Natural and Applied Sciences as a Master of Science thesis. 6 / June / 2024

Examining Committee Members (Institutions)

Signature

Chairman: Assist. Prof. Dr. Ferhat BOZDUMAN (KBU)

Member : Assist. Prof. Dr. Khalid Aal-SHABEEB (KBU)

Member : Assoc. Prof. Dr. Ali GÜLEÇ (ISUBU)

The degree of Master of Science by the thesis submitted is approved by the Administrative Board of the Institute of Graduate Programs, Karabuk University.

Assist. Dr. Zeynep ÖZCAN

Director of the Institute of Graduate Programs

“I declare that all the information within this thesis has been gathered and presented in accordance with academic regulations and ethical principles and I have according to the requirements of these regulations and principles cited all those which do not originate in this work as well.”

Mohammed Khairi Hussein HUSSEIN

ABSATRACT

M. Sc. Thesis

STUDYING THE EFFECT OF COLD PLASMA ON THE ETCHING PROCESS OF THE NUCLEAR TRACK DETECTOR CR-39.

Mohammed Khairi HUSSEIN

Karabük University

Institute of Graduate Programs

Department of Physics Natural and APPLIED Sciences

Thesis Advisor:

Assist. Prof. Dr. Ferhat BOZDUMAN

June 2024, 69 pages

In this work, cold plasma used in the process of etching the polymeric detector CR-39. This detector considered one of the important Nuclear Solid State Detectors because it used in many applications to measure the concentration of uranium, radon, and thoron in homes, soil, and food, in addition to many practical applications, such as its use to measure radiation doses. The detector used for detecting charged particles such as alpha particles, protons, and fission products, where the radiation works to disintegrate the polymer entanglement and break the bonds between the monomer, it passes to leave a track that is detected by using chemicals or using physical techniques such as electrochemical etching or using cold plasma. Therefore, the results recorded for using Argon plasma in etched the detectors. Radioactive source Americium-241 as the first group and Radium-226 as the second group, which emits alpha particles with different energy 5.485 and 4.485 MeV respectively. The results showed almost the same behavior, and this confirmed by calculation the

correlation coefficient, which showed that most of the etching cases are subject to a fifth-degree polynomial equation, also shown by the correlation coefficient of the results Plasma etching with chemical etching results were high, ranged 0.60 to 0.70. This means that we can rely on the plasma etching results and use the correlation process by choosing the most appropriate etching conditions, which showed a decrease in the number of tracks with increasing distance and reaching the maximum value of the curve at time of 40 and 30 minutes for the first and second groups respectively.

Key words :Nuclear trace detector CR-39, Argon cold plasma, Radon gas, Alpha particles, Track density, ^{226}Ra .

Science Code : 20219

ÖZET

Yüksek Lisans Tezi

YAZINIZ NÜKLEER İZ DEDEKTÖRÜ CR-39'UN AŞINMA SÜRECİ ÜZERİNDE SOĞUK PLAZMA ETKİSİNİN İNCELENMESİ.

Mohammed Khairi HUSSEIN

Karabük Üniversitesi

Lisansüstü Eğitim Enstitüsü

Fizik Anabilimdalı

Tez Danışmanı:

Öğr. Üyesi Ferhat BOZDUMAN

Haziran 2024, 69 sayfa

Bu çalışmada, polimerik dedektör CR-39'un aşındırılması işleminde soğuk plazma kullanıldı. Bu dedektör, önemli nükleer katı hal dedektörlerinden biri olarak kabul edilir çünkü evlerde, toprakta ve yiyeceklerde uranyum, radon ve toron konsantrasyonunu ölçmek için birçok uygulamada kullanılır. Radyasyon dozlarını ölçün. Radyasyonun polimer dolaşıklığını parçalamak ve monomer arasındaki bağları kırmak için çalıştığı alfa parçacıkları, protonlar ve fisyon ürünleri gibi yüklü parçacıkları tespit etmek için kullanılan dedektör, kimyasallar kullanılarak veya fiziksel olarak tespit edilen bir iz bırakmak için geçer. elektrokimyasal aşındırma veya soğuk plazma kullanımı gibi teknikler. Bu nedenle, kazınmış dedektörlerde Argon plazması kullanımına ilişkin sonuçlar kaydedildi. Birinci grup olarak radyoaktif kaynak Americium-241 ve ikinci grup olarak Radium-226, sırasıyla 5.485 ve 4.485 MeV farklı enerjiye sahip alfa parçacıkları yayar. Sonuçlar neredeyse aynı davranışı gösterdi ve bu, aşındırma durumlarının çoğunun beşinci derece bir polinom

denklemine tabi olduğunu gösteren korelasyon katsayısının hesaplanmasıyla doğrulandı ve aynı zamanda kimyasal aşındırma ile plazma aşındırma sonuçlarının korelasyon katsayısıyla da gösterildi. sonuçlar yüksekti, 0,60 ile 0,70 arasında değişiyordu. Bu, plazma aşındırma sonuçlarına güvenebileceğimiz ve en uygun aşındırma koşullarını seçerek korelasyon sürecini kullanabileceğimiz anlamına gelir; bu, mesafe arttıkça iz sayısında azalma olduğunu ve 40 ve 30° zamanlarında eğrinin maksimum değerine ulaştığını gösterir. Birinci ve ikinci grup için sırasıyla dakikalar.

Anahtar Sözcükler : Nükleer iz dedektörü CR-39, Argon soğuk plazma, Radon gazı, Alfa parçacıkları, İz yoğunluğu, ²²⁶Ra

Bilim Kodu : 20219

ACKNOWLEDGMENT

First, I thank Allah and praise Him for His countless blessings. He has the credit for putting me in this position and preferring me over many of His creation.

I extend my thanks and gratitude to my supervisor, Assist. Prof. Dr. Ferhat BOZDUMAN, who worked with me throughout the past period and provided me with all the advice and guidance for what I needed. He has my utmost appreciation and respect. I also extend my special thanks and gratitude to Asst. Prof. Dr. Khalid Hadi Mahdi Aal Shbeeb, who provided me with a lot of advice and was like a professor, teacher, and nurturing father. He has my sincere appreciation. Thank you to my family, friends, and everyone who supported and encouraged me throughout my studies.

I made my thanks and words at the end about love and tenderness, strength and safety, my mother and father, because words and thanks are long and never enough. Words are unable to express their blessing, and for all things they have been gave to me. Through my mother's prayers and my father's efforts, and after Allah, my success and excellence in my professional career achieved, I thank Allah and praise Him for His countless blessings. He has the credit for putting me in this place and favoring me over many of His creation.

CONTENTS

	<u>Page</u>
APPROVAL	ii
ABSTRACT	iv
ÖZET.....	vi
ACKNOWLEDGMENT.....	viii
CONTENTS.....	ix
LIST OF FIGURES.....	xi
LIST OF TABLES.....	xiii
SYMBOLS AND ABBREVIATIONS INDEX	xiv
PART 1	1
INTRODUCTION	1
1.1. PROBLEM STATEMENT	4
1.2. THE IMPORTANCE of the THESIS	4
1.3. AIMS and OBJECTIVES.....	6
PART 2	7
LITERATURE REVIEW	7
PART 3	10
THEORETICAL BACKGROUND.....	10
3.1. TYPES of the ETCHING PROCESS WITH NUCLEAR TRACK DETECTOR CR-39.....	10
3.2. TYPES of PLASMA	12
3.3. SOURCES of PLASMA GENERATION in NATURE	12
3.4. COLD PLASMA.....	14
3.5. TYPES AND METHODS OF GENERATING COLD PLASMA.....	14
3.7. APPLICATIONS of COLD PLASMA USING ARGON GAS.....	17
3.8. ARGON GAS	17
3.9. SOLID STATE NUCLEAR TRACK DETECTOR (CR-39).....	18

	<u>Page</u>
3.10. USES and PROPERTIES of TRACK DETECTOR CR-39.....	20
3.10.1. Uses of CR-39 Trace Detectors	20
3.10.2. Properties of CR-39 Trace Detectors.....	20
3.11. RADON GAS	21
3.11.1. Radon Gas Properties.....	23
3.11.2. Health Risks for Radon Gas.....	24
3.11.3. The Most Important Sources of Radon.....	25
3.12. ALPHA PARTICLES and THEIR ENERGY.....	26
PART 4	28
METHODOLOGY.....	28
4.1. EXPERIMENTAL SETUP.....	28
4.1.1. Plasma System Preparation	28
4.1.2. Irradiation of CR-39 Detectors	30
4.1.3. Etching by Plasma	30
4.2. RESULTS and DISCUSSION:.....	35
PART 5	60
CONCLUSION.....	60
REFERENCES.....	61
RESUME	69

LIST OF FIGURES

	<u>Page</u>
Figure 2.1. The Images (a) (b) (c)(d) show the effects of etching the CR-39 with Argon plasma[15] .	9
Figure 3.1. Use of cold plasma jet in a Covid-19 killing device [39].	15
Figure 3.2. The structural formula for the CR-39 trace detector [55].	19
Figure 4.1. Atmospheric pressure cold plasma setup.	29
Figure 4.2. Observing the waveform of the output signal with the help of an oscilloscope.	29
Figure 4.3. Argon cold plasma spectral lines.	30
Figure 4.4. An image the base in which the detector was placed when etching	32
Figure 4.5. An image of the plasma system that was used.	32
Figure 4.6. The argon bottle and meter used in the experiment.	33
Figure 4.7. An image of the power supply that was used.	33
Figure 4.8. Microscope used to detect antiquities.	34
Figure 4.9. Argon a plasma thermal camera images.	34
Figure 4.10. The track density with exposure time for a distance of (3) mm.	37
Figure 4.11. The track density with exposure time for a distance of (5) mm.	37
Figure 4.12. The track density with exposure time for a distance of (7) mm.	38
Figure 4.13. The track density with exposure time for a distance of (9) mm.	38
Figure 4.14. The track density with exposure time for a distance of (12) mm.	39
Figure 4.15. Etching effects for a distance of (3) mm and a time (a) 5 minutes (b) 10 minutes (c) 20 minutes (d) 30 minutes.	40
Figure 4.16. Etching effects for a distance of (3) mm with a time (a) 40 minutes (b) 50 minutes (c) 60 minutes and (d) for chemical etching (6 hours)	41
Figure 4.17. The correlation between results of chemical and plasma etching technique for Argon at D=3mm.	42
Figure 4.18. The correlation between results of chemical and plasma etching technique for Argon at D=5mm.	42
Figure 4.19. The correlation between results of chemical and plasma etching technique for Argon at D=7mm	43
Figure 4.20. The correlation between results of chemical and plasma etching technique for Argon at D=9mm.	43
Figure 4.21. The correlation between results of chemical and plasma etching technique for Argon at D=12mm	44

	<u>Page</u>
Figure 4.22. The fitting process for Argon gas at 3mm.	44
Figure 4.23. The fitting process for Argon gas at 5mm.	45
Figure 4.24. The fitting process for Argon gas at 7mm.	45
Figure 4.25. The fitting process for Argon gas at 9mm.	46
Figure 4.26. The fitting process for Argon gas at 12mm.	46
Figure 4.27. The relation between track density with distance at different time.	47
Figure 4.28. The track density with exposure time for a distance of (3) mm.	48
Figure 4.29. The track density with exposure time for a distance of (5) mm.	49
Figure 4.30. The track density with exposure time for a distance of (7) mm.	49
Figure 4.31. The track density with exposure time for a distance of (9) mm.	50
Figure 4.32. The track density with exposure time for a distance of (12) mm.	50
Figure 4.33. Etching effects for a distance of (3) mm and a time (a) 5 minutes (b) 10 minutes (c) 15 minutes (d) 20 minutes.	51
Figure 4.34. Etching effects for a distance of (3) mm with a time (a) 30 minutes (b) 40 minutes (c) 50 minutes and (d) for chemical etching (6 hours)	52
Figure 4.35. The correlation between results of chemical and plasma etching technique for Argon at D=3mm.	53
Figure 4.36. The correlation between results of chemical and plasma etching technique for Argon at D=5mm.	53
Figure 4.37. The correlation between results of chemical and plasma etching technique for Argon at D=7mm.	54
Figure 4.38. The correlation between results of chemical and plasma etching technique for Argon at D=9mm.	54
Figure 4.39. The correlation between results of chemical and plasma etching technique for Argon at D=12mm.	55
Figure 4.40. The fitting process for Argon gas at 3mm.	55
Figure 4.41. The fitting process for Argon gas at 5mm.	56
Figure 4.42. The fitting process for Argon gas at 7mm.	56
Figure 4.43. The fitting process for Argon gas at 9mm.	57
Figure 4.44. The fitting process for Argon gas at 12mm.	57
Figure 4.45. Change of trace detectors according to the relationship between time and distance.	58
Figure 4.46. The diameter of the track with the exposure time for Argon gas at 3mm-G1.	59
Figure 4.47. The diameter of the track with the exposure time for Argon gas at 3 ...	59

LIST OF TABLES

	<u>Page</u>
Table 4.1. Track density with time at different distances for Argon gas G1.....	36
Table 4.2. Track density with time at different distances for Argon gas G2.....	48
Table 4.3. The diameter of the track with the exposure time for each of the plasma.	58

SYMBOLS AND ABBREVIATIONS INDEX

SYMBOLS

Ar	:Argon
Na OH	: Sodium Hydroxide
KOH	: Potassium Hydroxide
N ₂	: Nitrogen
O ₂	: Oxygen

ABBREVIATIONS

SSNTD	: Solid State Nuclear Track Detector
DBD	: Dielectric Barrier Discharge
APPJ	: Atmospheric Pressure Plasma Jet
ICP	: Inductively Coupled Plasma
MIG	: metal inert gas
TIG	: tungsten inert gas
EPA	: Environmental Protection Agency
IARC	: The International Agency for Research on Canc

PART 1

INTRODUCTION

The discovery of radiation attributed to several key scientists and their groundbreaking experiments. Here are some of the significant milestones in the historical discovery of radiation.

The discovery of X-rays was by Wilhelm Conrad Rontgen (1895) [1]. In (1896) Henri Becquerel discovered radioactivity. Discovery of radioactive decay by Marie and Pierre Curie (1898) Marie and Pierre Curie, a Polish-French couple, worked extensively on radioactivity after Becquerel's discovery. In 1898, they announced that they had discovered polonium and radium, two highly radioactive elements, through the careful separation of radioactive ores. They also coined the term "radioactivity" to describe the property of certain elements to emit radiation spontaneously. Marie Curie went on to win two Nobel Prizes for her contributions to the study of radioactivity and the discovery of polonium and radium [2].

Development of the theory of radiation by Ernest Rutherford (early 20th century) Ernest Rutherford, a New Zealand-born physicist, conducted pioneering research on radioactive decay and the structure of the atom. Rutherford's suggestion of the concept of a nucleus within an atom led to the development of the nuclear model. His experiments, such as the famous gold foil experiment, provided evidence of their existence of alpha particles and the emission of radiation from the atomic nucleus. These discoveries collectively marked the foundation of the field of radiation science. Subsequent research by numerous scientists further expanded our understanding of radiation, including different types of radiation (Alpha, Beta, Gamma), their properties, and their effects on matter and living organisms. The study of radiation has had significant impacts on fields such as medicine, energy production, materials science, and nuclear physics [3] .

CR-39 is a type of solid-state nuclear track detector (SSNTD) commonly used for radiation detection and analysis. It is a transparent polymer material composed of poly-allyl di-glycol carbonate. CR-39 detectors are widely used in various fields, including radiation dosimetry, particle physics, nuclear engineering, and environmental monitoring

CR-39 detectors offer a versatile and reliable method for radiation detection, characterization, and dosimetry across various scientific and industrial applications. Their unique properties make them valuable tools for studying radiation effects, monitoring radiation exposure, and advancing our understanding of the interaction of charged particles with matter [4].

Cold plasma, also known as non-equilibrium plasma or atmospheric plasma refers to a state of plasma where the gas temperature remains relatively low, typically close to room temperature, while the electrons in the plasma have higher energy levels. Plasma often referred to as the fourth state of matter and created by ionizing a gas through the application of energy.

In cold plasma, the gas is ionized by various methods such as electrical discharges, electromagnetic fields, or exposure to intense light. Unlike high-temperature plasmas, such as those found in stars or fusion reactors, cold plasma does not require significant heating of the gas. The low gas temperature allows for a wide range of applications in various fields, including medicine, material science, agriculture, and environmental engineering [5].

Cold plasma treatment commonly used to enhance the sensitivity of CR-39 detectors for detecting and analyzing charged particles. The choice of gas in the cold plasma can affect the etching process and the subsequent track formation on the CR-39 surface. Different gases can have varying chemical reactivities and etching properties, which can affect the track characteristics.

For example, commonly used gases in cold plasma treatments include oxygen (O₂), nitrogen (N₂), and argon (Ar). Oxygen plasma known to provide high etching selectivity for tracks, resulting in well-defined and clear tracks. Nitrogen plasma, on

the other hand, tends to produce tracks with larger diameters and a higher degree of etching-induced damage. Argon plasma can have intermediate effects on the etching process.

The choice of gas should be based on the specific requirements of the experiment or application. It is essential to consider the desired track characteristics, track density, and other factors relevant to the analysis [6].

Alpha energy, also known as alpha particle energy or alpha particle kinetic energy, refers to the amount of energy carried by an alpha particle. An alpha particle is essentially the nucleus of a helium atom, which is a type of ionizing radiation consisting of two neutrons and two protons. It is represented by the symbol α .

The alpha energy is determined by the kinetic energy of the alpha particle as it moves through space. This energy depends on factors such as the initial velocity of the particle, its mass, and any interactions or collisions it experiences along its path [7].

The kinetic energy of an alpha particle can be calculated using the equation:

$$E = \frac{1}{2}mv^2$$

Where v is alpha velocity, E is the kinetic energy, and m is the mass of the alpha particle. Since the mass and charge of an alpha particle are known (approximately 6.644×10^{-27} kilograms and twice the elementary charge, respectively), the kinetic energy can be determined if the velocity is known.

The alpha energy can vary depending on the source of the alpha particles. For example, naturally occurring radioactive materials such as uranium and thorium decay, and emit alpha particles as part of their radioactive decay process. The alpha energies associated with these decays can range from a few MeV (mega-electron volts) up to several MeV [8].

Radon gas is a colorless, odorless, and tasteless gas, making it difficult to detect without specific testing. It is a radioactive gas, which occurs naturally from the decay of thorium and uranium in the rocks, soil, and water [9].

This research aims to develop a new method in etching trace detector CR-39 using Argon plasma non-thermal produced at normal atmospheric pressure.

1.1. PROBLEM STATEMENT

The impact of radon gas (which emits alpha radiation) and other natural sources on the environment and the dangers they cause to humans prompted researchers to study and develop etching processes for the CR-39 polymeric nuclear path detector used to detect alpha paths emitted from various sources, such as chemical etching and other etching processes. In this research, we will work to develop the use of non-thermal argon plasma in performing the etching process for the polymer detector irradiated with two alpha ray sources with two (^{226}Ra and ^{241}Am) with different energies and the suitability of working with the conditions associated with the plasma system and the detector.

1.2. THE IMPORTANCE of the THESIS

Studying the effect of cold plasma on the etching process of the nuclear track detector CR-39 is important for several reasons:

1. Optimal track formation: The type of gas used in the cold plasma can influence the etching process and subsequent track formation on the CR-39 detector. Different gases have varying chemical reactivities and etching properties, which can affect the track characteristics such as track diameter, depth, and shape.
2. Control of track properties: The distance between the cold plasma source and the CR-39 detector can also effect the etching process and track properties. Controlling the distance allows researchers to regulate the energy and density of plasma species reaching the detector surface. This control is crucial for achieving desired track characteristics, such as track density, size, and

uniformity. By studying the effect of distance, researchers can optimize the drilling process to obtain consistent and reproducible track properties.

3. Performance enhancement: Understanding the influence of energy of Alpha particle on the etching process by cold plasma can help improve the performance of CR-39 detectors. By optimizing the etching process, researchers can enhance the sensitivity, efficiency, and accuracy of the detectors. This is particularly important in applications where precise track detection and analysis are required, such as in radiation dosimetry, particle physics, and nuclear engineering.
4. Tailored applications: Different applications may have specific requirements for track characteristics. For example, in particle physics experiments, clear and well-defined tracks are desirable for accurate particle identification and energy determination. On the other hand, environmental monitoring applications may require higher track densities to detect and analyze low-energy particles. By this work, researchers can tailor the etching process to meet the specific needs of different applications.
5. Process optimization and cost-effectiveness: Studying the drilling process parameters can lead to process optimization, reducing costs and improving efficiency. By understanding the relationship between energy of radiation, distance, and track formation, researchers can identify the optimal conditions that maximize the etching efficiency while minimizing resources and time required for the drilling process. Overall, studying the effect of energy of radiation and the distance with the detector on the etching process using cold plasma. It is important for achieving optimal track formation, controlling track properties, enhancing performance, tailoring applications, and optimizing the process as well as in this research reducing the time from 6 hours or more, as in chemical etching, to a few minutes. This knowledge contributes to the advancement of research and applications involving CR-39 detectors and enables more accurate and reliable measurements of charged particle interactions.

1.3. AIMS and OBJECTIVES

Therefore, in this work, a modern method is used for etching the nuclear track detector CR-39. Which is cold argon plasma at normal atmospheric pressure, and showing the effect of the energy of radiation (with specific conditions) in the etching process and on nuclear track density and nuclear track diameter and their relationship with plasma exposure time. The possibility of applying them to different detectors and different energies for radiation.

PART 2

LITERATURE REVIEW

1. **Salim M.D. et.al, (2020)** study the etching parameters using three types of solid-state nuclear track detectors (PM-355, CR-39 and LR-115). Five techniques used to heat the etchant chemical, dry etching technique (plasma), microwave, water bath, thermal oven, and ultrasound. After the three nuclear track detectors exposed to the alpha energy emitted from the element radium-226, it was found in this study that the best time to drill the CR-39 detector was for plasma was (50sec), for a microwave was (10min), a water bath , for a thermal oven was (90min) and for ultrasonic cleaner was (90-120min)[10].
2. **Oliveira C.S. et.al ,(2021)** , as a function of chemical etching time, in this study, the efficiency of two available CR-39 plastic detectors studied, type Baryotrak and Lantra . For density curves as well as to build etch pit diameter growths, and at a temperature of 70 and 80 °C, using chemical etching solutions of KOH, NaOH and ethyl alcohol NaOH. After that, at 70 °C, and by comparing the results of growth curves previously obtained for the etch pit diameters, similar trends were shown for the Baryotrak and Lantrak detectors. At 80 °C, a slight divergence of the curves seen for etching times of more than 400 minutes, which led to the emergence of a difference in the largest etching rates between both types of detectors [11, 12].

3. **Ahmed A.I. & Wathab H.Y. (2018)**, studied a number of etching detectors as well as the effect of two types of chemical etching solutions on the properties of the solid nuclear track detector CR-39. The first type of solution resulting from dissolving NaOH in (water + Ethanol) prepared under different natural conditions, then the second type prepared from the solution resulting from dissolving NaOH in water (NaOH/water), after that a comparison was made between the two types at different temperatures and different natural conditions [13].

4. **Kravets L.I. et.al (2018)**, study the electrochemical and surface characteristics of a polypropylene track etched membrane treated with oxygen, air and nitrogen plasma. They found that the effect of non-polymerized plasma gas forms groups containing Oxygen, most of which are carboxyl and carbonyl. In addition, a change found in the micro-relief of the membrane surface formed under the gas discharge etching [14].

5. **Hamid H. M. et.al (2016)**, used the plasma jet system and designed at atmospheric pressure in a laboratory, the voltage of the plasma system was (6) kilowatts, and at a frequency of (12) kilohertz, argon gas used to feed the system. At a flow rate of 3 liters per minute for etching the nuclear track detector CR-39 instead of chemical etching [15]. Figure 2.1 show the plasma effect on nuclear track detectors in etching process for this study.

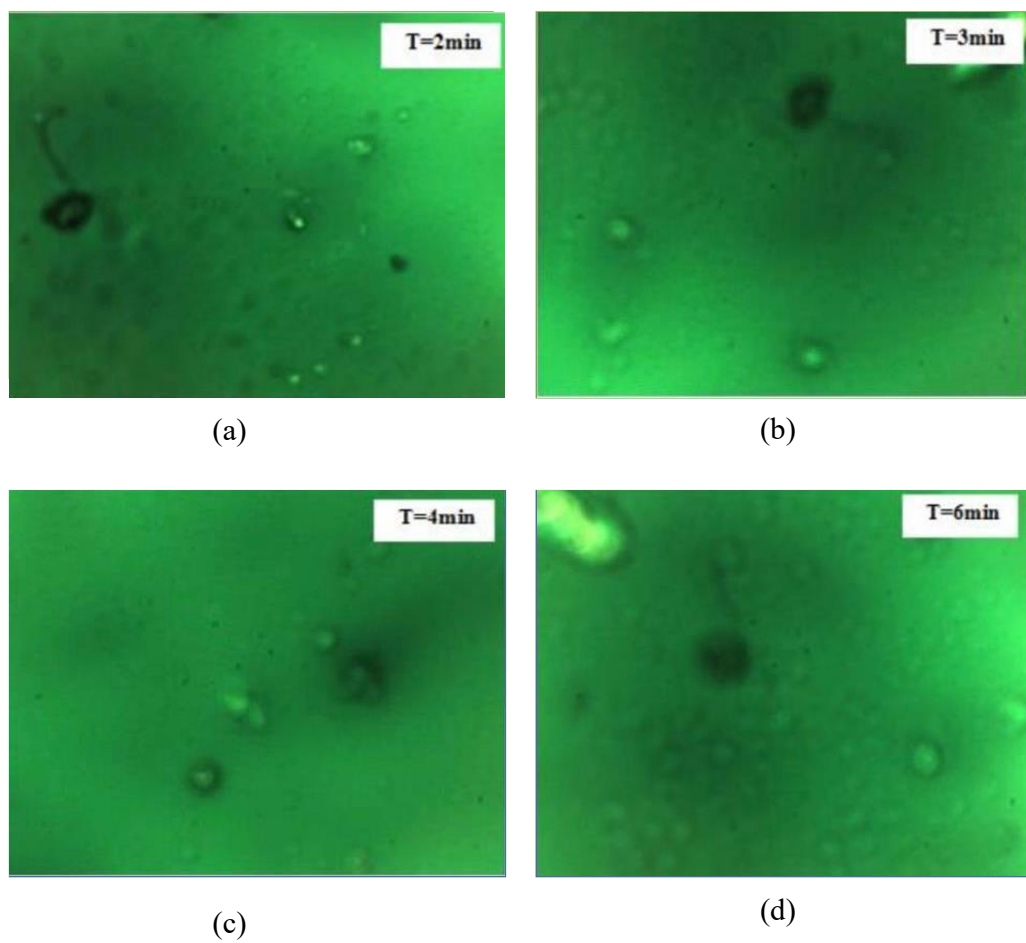


Figure 2.1. The Images (a) (b) (c)(d) show the effects of etching the CR-39 with Argon plasma[15] .

PART 3

THEORETICAL BACKGROUND

The studies in the previous chapter showed that the results of this research are very important and useful for understanding the whole problem. This section provides an overview of studying the effect of the energy of radiation in etching process when we used the cold plasma on the distance between the detector and plasma jet, number, diameter of the tracks in the nuclear track detector CR-39.

3.1. TYPES of the ETCHING PROCESS WITH NUCLEAR TRACK DETECTOR CR-39

There are many different processes and methods of the etching nuclear track detector (CR-39), and below we will mention a number of them:

1. **Chemical Etching:** Chemical etching is the most common and widely used method for CR-39 detectors. It involves immersing the CR-39 detector in a suitable etching solution, typically concentrated sodium hydroxide (NaOH) or potassium hydroxide (KOH), at an elevated temperature. The etching solution selectively removes the polymer material around the damaged regions caused by charged particles, enlarging the tracks and making them visible under a microscope. The etching process is highly controlled, and the track size and shape can be adjust by varying the etching time, temperature, and concentration of the etching solution.**Electrochemical Etching:** Electrochemical etching is an alternative method for etching CR-39 detectors. It involves applying a voltage between the CR-39 detector and a counter electrode while they immersed in an electrolyte solution. The applied voltage induces localized electrochemical reactions, leading to the selective removal of polymer material and the formation of tracks. Electrochemical etching

offers some advantages, such as better control over the etching process and the ability to etch specific areas or patterns on the detector surface [16].

2. **Laser Etching:** Laser etching is a more specialized and precise method for etching CR-39 detectors. In this technique, a focused laser beam is used to ablate the polymer material around the tracks, revealing the tracks' latent damage. Laser etching allows for higher spatial resolution and the possibility of selectively etching specific tracks or regions of interest. It is often used in research applications requiring detailed analysis of individual tracks or for studies where specific track patterns are of interest [17].
3. **Etching by Cold plasma:** At the present time, various sources have been developed to produce non-thermal plasma at normal atmospheric pressure in order to use it to treat the surfaces of materials [18]. This type of plasma, if we compare it with other surface treatment methods, has many advantages when using it, such as the use of plasma, the use of chemicals, or the use of chemicals produced at low pressure. Among these advantages are, for example, shorter processing time, lower maintenance and operating costs, and the absence of toxic materials or wastes. Extensive studies have been performed on the effect of non-thermal plasmas on surfaces of polymers [19], textiles [20], or plastics [21] at atmospheric pressure. When surface modifications are necessary to overcome some technological problems in materials, such as increasing adhesion or reducing surface moisture. Compared to the number of studies conducted on the effect of non-thermal plasma on polymer surfaces, and has been studied on metallic surfaces, compared to the number of studies conducted on the effect of non-thermal plasma on polymer surfaces, but to a lesser extent, and much work still needed. In this topic [22]. There are a large number of published researches on the use of plasma to treat metal surfaces, whether cleaning or revitalizing them.

3.2. TYPES of PLASMA

Below are some types of plasma briefly:

1. Thermal plasma: This type of plasma characterized by high temperatures, usually reaching thousands or tens of thousands of degrees Celsius. These plasmas are often use in applications such as welding, cutting, and some industrial processes [23].
2. Non-thermal or cold plasma: In non-thermal plasma or also cold plasma, the temperatures lower compared to thermal plasma. It has many uses in different applications, including surface treatments, sterilization, and medical applications [24].
3. Magnetic plasma: Magnetic plasma has an important role in magnetic fields in its behavior and dynamics, and magnetized plasma greatly affected by magnetic fields. These plasmas often studies in the context of fusion research, where magnetic confinement used to control and stabilize the plasma [25].
4. Astrophysical plasma: Astrophysical plasma characterized by very high densities and temperatures, and found in celestial bodies. Examples of this are solar plasma and the plasma found in the interior parts of stars [26].
5. Dusty Plasma: Dusty plasma contains small solid particles (dust grains) as well as ions and electrons. They have been study in laboratories, and found in certain astrophysical environments [27].

3.3. SOURCES of PLASMA GENERATION in NATURE

Plasma exists in various natural phenomena. Here are some natural sources of plasma in nature:

1. Stars: The most prominent natural source of plasma is stars, including our Sun. The immense heat and pressure at the core of stars cause the atoms to lose their electrons, creating a high-temperature plasma. The Sun, for example, is a ball of ionized gas, primarily consisting of hydrogen and helium in a plasma state [28].
2. Lightning: Lightning is a natural electrical discharge that occurs during thunderstorms. The high voltage difference between the ground and the atmosphere ionizes the air, creating a conducting path for the electrical discharge. The visible flash of lightning is a plasma channel [29].
3. Auroras: Auroras, such as the Northern and Southern Lights, produced when charged particles from the solar wind interact with the Earth's magnetic field. The collisions between these charged particles and atmospheric gases result in the emission of light, creating colorful displays. The ionization of gases in the upper atmosphere forms plasma that contributes to the visual spectacle [30].
4. Flames: Flames from sources like candles, forest fires, or gas stoves consist of hot gases in a plasma state. The heat causes the ionization of atoms and molecules in the fuel, creating a luminous plasma that emits light [31].
5. Ionospheres Plasma: The Earth's ionosphere is a region of the upper atmosphere where solar radiation ionizes atoms and molecules. This ionization results in a plasma layer that plays a crucial role in the reflection of radio waves and the formation of the ionospheres' currents [32].
6. Magnetosphere Plasma: The Earth's magnetosphere contains plasma created by the interaction of the solar wind with the Earth's magnetic field. This plasma is responsible for phenomena such as the Van Allen radiation belts and contributes to the dynamics of space weather [33].

3.4. COLD PLASMA

Cold plasma refers to a partially ionized gas state where the gas remains close to room temperature despite containing a significant population of charged particles (ions and electrons). It called "cold" plasma to distinguish it from high-temperature plasmas generated in fusion reactors or stars .The presence of charged particles in the gas gives cold plasma its unique properties. It exhibits characteristics of both gases and plasmas. Cold plasma can conduct electricity and respond to electromagnetic fields due to the presence of charged particles, but it retains some of the properties of a gas, such as its density and viscosity [34].

3.5. TYPES AND METHODS OF GENERATING COLD PLASMA

There are several types of cold plasma, each with its unique characteristics and applications. Here are some commonly encountered types of cold plasma:

1. **Glow Discharge Plasma:** Glow discharge plasma is one of the most common types of cold plasma. It generated by applying a voltage across two electrodes placed in a gas at low pressure. The gas is partially ionized, and the resulting plasma emits a visible glow. Glow discharge plasma is widely used for various applications, including surface cleaning, thin film deposition, and plasma etching [35].
2. **Dielectric Barrie Discharge** is a type of plasma discharge that occurs between two electrodes separated by a dielectric material (an insulator). It a non-thermal plasma process that has various applications in fields such as surface treatment, air purification, and material modification. DBD plasma often operated at atmospheric pressure, making it suitable for applications such as surface modification, sterilization, and pollutant degradation [36].

3. Corona Discharge Plasma: Corona discharge plasma created by applying a high voltage to a pointed electrode or a thin wire electrode in a gas at atmospheric pressure. The electric field at the electrode causes ionization and the formation of a corona discharge. Corona discharge plasma commonly used in air purification systems, ozone generation, and electrostatic precipitation [37].

4. Atmospheric Pressure Plasma Jet (APPJ): is a type of plasma source that operates at or near atmospheric pressure, meaning it functions under the same pressure conditions as the surrounding air. This is in contrast to many traditional plasma sources that require vacuum conditions for operation. The APPJ generates a plasma discharge in a focused and directed manner [38].

5. Plasma jet often resembling a narrow jet or plume of plasma. This technology has various applications in fields such as materials processing, surface treatment, medicine, and more. It involves directing a plasma jet toward a target surface [38].

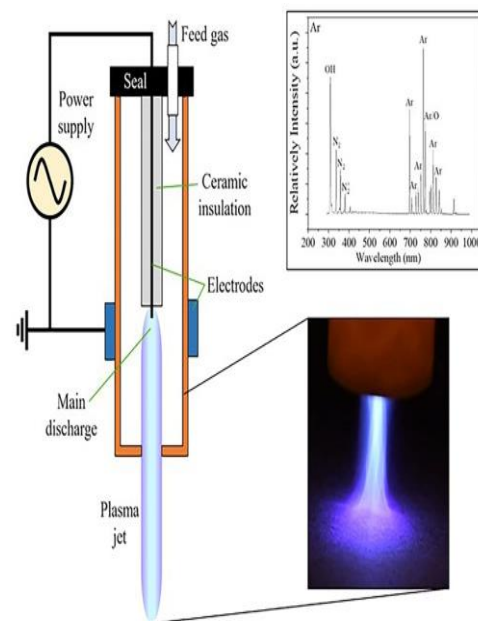


Figure 3.1. Use of cold plasma jet in a Covid-19 killing device [39].

6. Inductively Coupled Plasma (ICP): is a type of high-temperature plasma source that widely used for elemental analysis, spectroscopy, and various applications in analytical chemistry, materials science, and environmental monitoring. ICP characterized by its ability to ionize samples at high temperatures, leading to efficient atomization and excitation of atoms and ions. It involves using a coil to generate a strong magnetic field that induces plasma formation in a gas [40].

7. Electrical Discharge: In this method, a high voltage applied to a gas to create an electric field. When the electric field exceeds a certain threshold, the gas becomes ionize, forming a plasma. Electrical discharge methods include:
 - a. Direct Current (DC) Discharge: A direct current passed through the gas to generate plasma [41].
 - b. Radiofrequency (RF) Discharge: An alternating current at radiofrequency used to create plasma [42].
 - c. Microwave Discharge: Microwaves used to generate plasma in a resonant cavity [43].

8. Argon cold plasma: Cold plasma can be produce using argon gas by subjecting the gas to an electric or electromagnetic field at low pressure. This process creates a low-temperature, non-thermal plasma with a variety of reactive species, such as ions, electrons, and free radicals .The setup usually involves a plasma chamber or reactor, which is a vessel designed to contain the argon gas at low pressure. Argon gas injected into the plasma chamber to create the plasma medium. The pressure inside the chamber reduced to create a low-pressure environment. The pressure is typically in the range of a few mill bars to a few tens of mill bars. An electric or electromagnetic field applied to the argon gas in the chamber. This can be achieve through various methods, such as radiofrequency (RF) or direct current (DC) power supplies .

The applied electric or electromagnetic field excites the argon atoms in the gas, causing them to ionize and generate a plasma state. Reactive Species Formation: In the low-temperature plasma, some argon atoms become ionized, creating positively charged argon ions (Ar^+). Electrons also freed from the argon atoms, creating a cloud of electrons. Additionally, various reactive species, such as free radicals and metastable states, are formed during the plasma process [44, 45, 46].

3.7. APPLICATIONS of COLD PLASMA USING ARGON GAS

Cold plasma generated using argon gas finds applications in various fields, including:

1. **Surface Cleaning and Modification:** Cold plasma used for surface cleaning and activation of materials before bonding or coating processes.
2. **Sterilization and Decontamination:** Cold plasma can be utilized for the sterilization of medical instruments and decontamination of surfaces.
3. **Materials Synthesis:** Cold plasma used for the synthesis of nanostructured materials and thin films [47].
4. **Medical Treatments:** Cold plasma explored for medical applications, such as wound healing and cancer treatment.
5. **Argon plasma used to eliminate the Covid-19 virus, as well as get rid of insects and bacteria [48].**

3.8. ARGON GAS

Argon gas is a chemical element that belongs to the noble gases group in the periodic table of elements. Argon gas is represented by the chemical symbol "Ar", and is an odorless, colorless, and tasteless gas. Argon is indeed an inert gas, which means that

it is chemically unreactive under normal conditions. Inert gases, also known as noble gases, are a group of elements on the periodic table that have a full complement of electrons in their outermost electron shell. This configuration makes them highly stable and unlikely to form chemical compounds with other elements. Argon is the third most abundant gas in Earth's atmosphere, following nitrogen and oxygen. It accounts for a significant portion of the atmosphere's composition, earth's atmosphere primarily composed of nitrogen (about 78%) and oxygen (about 21%). However, a small fraction of the atmosphere (around 0.934%) is composed of noble gases, including argon. Among these noble gases, argon is the third most abundant, after helium and neon. Argon classified as a noble gas due to its stable and unreactive nature. It does not readily form chemical compounds with other elements, making it chemically inert. Argon is non-flammable and does not support combustion. It considered safe for use in various applications. One of the most common and important uses of argon gas is in welding processes. Argon used as a shielding gas in metal inert gas (MIG) welding and tungsten inert gas (TIG) welding to protect the welding area from atmospheric contamination, preventing oxidation and ensuring high-quality welds. Besides its use in gas-discharge lamps, argon gas also used in fluorescent tubes and other lighting technologies to facilitate the discharge of electricity and produce light [49, 50, and 51].

3.9. SOLID STATE NUCLEAR TRACK DETECTOR (CR-39)

A Solid State Nuclear Track Detector (CR-39) is a type of passive radiation dosimeter that used to detect and measure ionizing radiation. It consists of a solid material, often a polymer, which is sensitive to high-energy charged particles. The principle operation of detector based on, when these particles pass through the material, they create damage tracks or latent tracks that can be etch and made visible for analysis. The detector material is usually a polymer. The detector material is usually a polymer with a high atomic number, such as polycarbonate (like CR-39) or polyester. These materials have a dense arrangement of atoms that makes them sensitive to the passage of high-energy charged particles. When the (CR-39) exposed to ionizing radiation, such as alpha particles, beta particles, or heavy ions, these particles penetrate the material and cause damage along their paths. This damage

disrupts the molecular structure of the material. The damaged regions along the particle's path act as sites for further chemical etching. When the detector immersed in a suitable etching solution, the damaged tracks become visible as etched tracks. Each track corresponds to the path of an individual particle that passed through the material. The number, density, and characteristics of the etched tracks provide information about the type and energy of the incident radiation. These tracks can be count and measure under a microscope or through automated image analysis. Solid State Nuclear Track Detectors have various applications, including radiation dosimetry, particle detection nuclear physics research [52, 53] . The Columbia Resin 39 (CR-39) Solid State Nuclear Track Detector (SSNTD) discovered and developed in the 1960s. It created by the Columbia University Radiation Laboratory as a material for detecting and recording the tracks of high-energy charged particles, particularly alpha particles. Since then, CR-39 detectors have found numerous applications in various scientific and industrial fields due to their effectiveness in detecting and recording the paths of charged particles like alpha particles. [54]. Figure (3-1) shows the CR-39 detector assembly

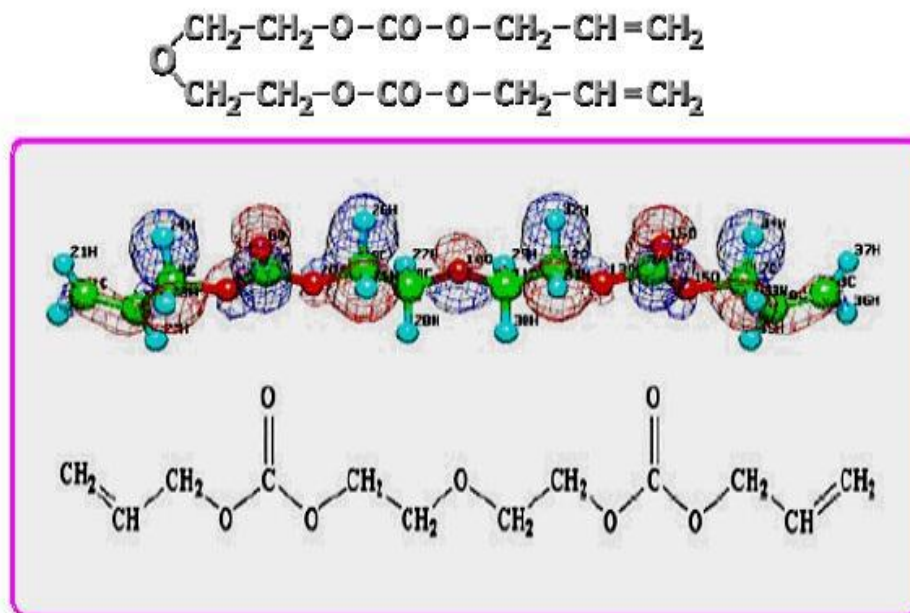


Figure 3.2. The structural formula for the CR-39 trace detector [55].

3.10. USES and PROPERTIES of TRACK DETECTOR CR-39

The CR-39 (Columbia Resin 39) detector, a type of Solid State Nuclear Track Detector (SSNTD), primarily used for detecting and recording the tracks of charged particles resulting from ionizing radiation. Here are some common uses and properties of trace detectors CR-39:

3.10.1. Uses of CR-39 Trace Detectors

1. Radon Gas Detection: CR-39 detectors are widely used to measure and monitor indoor radon gas levels, which can be a health hazard if present in high concentrations [56].
2. Nuclear Physics Experiments: CR-39 detectors used in various nuclear physics experiments to study charged particle interactions and nuclear reactions.
3. Space Missions and particle Identification: In high-energy physics outside the Earth's atmosphere and cosmic ray research, CR-39 detectors used for particle identification and track measurements [57].
4. Neutron Dosimetry: CR-39 detectors can be combine with appropriate converters to measured neutron radiation levels [58].
5. Environmental Monitoring: CR-39 detectors used for environmental monitoring to detect alpha particles and heavy ions released from natural or anthropogenic sources [59].

3.10.2. Properties of CR-39 Trace Detectors

CR-39 detectors are highly sensitive to alpha particles and heavy ions, making them suitable for detecting low-energy and low-intensity radiation. The tracks formed on

the CR-39 detector's surface are permanent and do not fade over time, allowing for long-term analysis. CR-39 detectors are primarily sensitive to charged particles (alpha and heavy ions) and are relatively insensitive to beta and gamma radiation. CR-39 detectors can be chemically etched to reveal and enlarge the tracks, making them visible and suitable for analysis under a microscope. CR-39 detectors offer high spatial resolution, allowing for detailed measurements and analysis of particle tracks. CR-39 detectors typically have low background noise, enabling accurate detection of radiation-induced tracks. CR-39 detectors are relatively inexpensive compared to other radiation detectors, making them an attractive option for various research and monitoring applications. CR-39 detectors are passive detectors that do not require an external power source, making them suitable for long-term monitoring and remote applications. The unique properties of CR-39 detectors make them valuable tools in various radiation detection and particle tracking applications. Their simplicity, reliability, and cost-effectiveness contribute to their widespread use in scientific research, environmental monitoring, and nuclear physics experiments [56, 60].

3.11. RADON GAS

Radon is one of the naturally radioactive noble gases. It is formed through the radioactive decay of thorium and uranium, which are found in varying amounts in the Earth's crust. Uranium and Thorium decay over time, releasing radon gas isotopes as one of their decay products. It cannot be detected by human senses. It is a part of the radioactive decay chain of these elements and is considered a health concern due to its potential to accumulate in indoor spaces and pose health risks to humans. It is chemically inert, which means it does not readily react with other substances. Prolonged exposure to elevated levels of radon gas is associated with an increased risk of lung cancer. Radon is considered the second leading cause of lung cancer after smoking [61].

The history of radon gas begins with the discovery of radioactivity in the late 19th and early 20th centuries. Here is a brief timeline of the key events in the history of radon gas. In (1895), discovery of X-rays. German physicist Wilhelm Conrad

Roentgen discovers X-rays, a form of ionizing radiation, which opens the door to the study of radioactivity [62].

In 1896, discovery of radioactivity. French physicist Henri Becquerel discovered natural radioactivity, while studying the fluorescence of uranium salts. He found that uranium minerals emit radiation without external excitation [63].

In 1900, discovery of Radon. German physicist Friedrich Ernst Dorn discovered radon gas, while studying the radioactive decay of radium. He observed the presence of a radioactive gas emitted by radium, which he names "radon"[64].

From 1910s to 1920s, identification of Radon Progeny. Ernest Rutherford and others identified that radon gas decays into other radioactive isotopes known as "radon progeny" or "radon daughters." In (1930s), health effects of Radon. Studies begin to show an association between exposure to radon and lung cancer, particularly among uranium miners. However, the full health implications of radon exposure were not yet fully understood [65].

From 1940s to 1950s, Radon in Buildings became apparent, that radon gas can accumulate in indoor spaces, particularly in underground mines, caves, and buildings with poor ventilation. From 1960s to 1970s, further Health Studies. Studies of uranium miners and other underground workers continue to show increased lung cancer risks associated with radon exposure. At period 1970s to 1980s, public awareness. Radon gains increasing public attention as a potential health hazard. Government agencies and health organizations begin to address radon as an indoor air quality concern. In (1984) EPA Guidance. The U.S. Environmental Protection Agency (EPA) issues guidance on radon mitigation and radon-resistant construction techniques. (1988) Radon as a Carcinogen - The International Agency for Research on Cancer (IARC) classified radon as a Group 1 carcinogen, recognizing it as a cause of lung cancer in humans. From 1990s until Present, Radon Regulations. Many countries develop regulations and guidelines for indoor radon levels and encourage radon testing and mitigation in homes and workplaces.

Today, radon gas continues to be a significant concern for indoor air quality and public health. Efforts are ongoing to raise awareness, test for radon levels in indoor spaces, and implement mitigation measures to reduce radon exposure and associated health risks [66].

3.11.1. Radon Gas Properties

These are some of the properties of radon gas:

1. **Radioactivity:** Radon is radioactive, and it emits ionizing radiation in the form of alpha particles, beta particles, and gamma rays. This radioactivity is the primary reason for its health risks [67].
2. **Density:** Radon is denser than air, with a density approximately 9 times that of air. As a result, it tends to accumulate in low-lying areas, such as basements and crawl spaces [68].
3. **Solubility:** Radon is moderately soluble in water. It can dissolve in water, and in some areas, it can be released into the air from water sources, such as wells and springs [69].
4. **Decay Chain:** Radon undergoes a series of radioactive decay processes, forming different radioactive isotopes known as radon decay products or radon progeny. These decay products, such as polonium and lead isotopes, are also radioactive and can attach to dust and airborne particles [70].
5. **Half-Life:** Radon has a relatively short half-life, with the most common isotope, radon ^{226}Ra , having a half-life of about 3.8 days. This means that radon levels decrease relatively quickly over time [71].
6. **Health Risks:** Radon gas is a known human carcinogen. When inhaled, its decay products can deposit in the lungs and emit alpha particles, which can damage lung tissue and increase the risk of developing lung cancer, especially in long-term exposures [72].

7. Migration: Radon can migrate from the ground and enter homes and buildings through cracks and openings in the foundation. Elevated radon levels indoors can pose health risks to occupants [73].
8. Radon Levels: Radon concentrations measured in Becquerel per cubic meter (Bq/m³) or picocuries per liter (pCi/L). The World Health Organization (WHO) and many health authorities recommend action levels below 100 Bq/m³ (2.7 pCi/L) for indoor radon [74].

3.11.2. Health Risks for Radon Gas

Radon gas poses significant health risks, primarily due to its radioactive nature and the potential for long-term exposure. Lung cancer is one of the most common diseases resulting from prolonged exposure to radon gas [75, 76].

Exposure to high levels of radon gas for long periods increases the risk of lung cancer, especially in individuals who smoke or have a history of smoking. Radon is second only to smoking in causing lung cancer. It is estimated to be responsible for thousands of lung cancer deaths worldwide each year. The combination of smoking and radon exposure significantly amplifies the risk of lung cancer. Radon exposure poses a higher risk of lung cancer for non-smokers compared to that from smoke. Non-smokers who are exposed to high levels of radon also greatly increase their risk of developing lung cancer over their lifetime. Radon can enter homes and buildings from the ground through cracks and openings in the foundation. Indoor radon levels can vary based on factors such as geology, construction, ventilation, and lifestyle habits. Long-term exposure to elevated radon levels indoors can lead to an increased risk of lung cancer among occupants [77, 78]. Radon is odorless, tasteless, and colorless, which means it cannot be easily detected with simple tools or human senses. As a result, there are no immediate symptoms or signs of radon exposure, making it a silent health risk. The health effects of radon exposure may not manifest immediately. The development of lung cancer due to radon exposure typically occurs over many years, with a latency period of 5 to 25 years or more. Certain occupations,

such as uranium miners and workers in underground spaces, may face higher radon exposure levels and an increased risk of lung cancer [79, 80, and 81]. Radon gas can have several effects on the environment, particularly when it released into the air and water. Radon gas is a natural radioactive pollutant. When released into the atmosphere, it can contribute to air pollution. However, the overall contribution of radon to air pollution is relatively small compared to other sources [82]. Decay of radon decay products can contribute to the formation of ground-level ozone. The secondary pollutant is ozone, which can harm human health and the environment, in the form of smog in particular [83].

3.11.3. The Most Important Sources of Radon

The most important sources of radon emissions related to the natural decay of radioactive elements found in the Earth's crust. Radon is a naturally occurring gas produced by the radioactive decay of radium, which is a decay product of uranium and thorium [84]. Here are the primary sources of radon emissions:

1. **Soil and Rocks:** The soil and rocks in the Earth's crust contain varying amounts of uranium and thorium. As these radioactive elements decay, they produce radon gas. Radon can migrate from the ground into the air and enter buildings, resulting in indoor radon levels.
2. **Building Materials:** Some building materials, particularly those containing naturally occurring radioactive elements like uranium and thorium, can emit radon gas indoors. Common examples include concrete, brick, and certain types of stones [85].
3. **Radioactive Waste and Tailings:** Certain industrial activities, such as uranium mining and milling, can produce large amounts of radioactive waste and tailings containing uranium and thorium. These materials can release radon gas into the environment if not managed properly [86].

4. Natural Gas: Natural gas extracted from the ground can contain trace amounts of radon. When natural gas burned for heating, cooking, or electricity generators, radon can be release into the outdoor air [87].
5. Groundwater: Radon can dissolve in groundwater, and when water used or disturbed, radon can be release into the indoor air. Well water, in particular, can be a source of indoor radon emissions [88].
6. Geothermal Sources: In areas with geothermal activity, such as hot springs and geysers, radon emissions can occur due to the presence of radioactive elements in the geothermal fluids [89].

3.12. ALPHA PARTICLES and THEIR ENERGY

Alpha particles consist of two protons and two neutrons, making it a helium-4 nucleus. The emitted alpha particle carries energy and momentum, and travels very quickly. It is also a type of ionizing radiation. As it passes through matter, it interacts strongly with atoms and molecules, causing ionization by stripping electrons from them. This ionization can disrupt chemical bonds and potentially damage biological tissue if alpha-emitting substances are present within the body. They are relatively heavy and large compared to other types of radiation, such as beta particles or gamma rays [90]. During the decay process of radium ^{226}Ra , alpha particles emitted. Alpha decay involves the expulsion of an alpha particle from the nucleus of a radon atom [91]. Alpha particles emitted by radon and its decay products are a major cause of the potential health risks associated with radon exposure. These alpha particles can cause ionization and cellular damage in lung tissue, contributing to an increased risk of lung cancer [92]. Alpha particles widely used in a variety of scientific and industrial applications. These applications take advantage of the large interaction force and strong radiation that alpha particles emit. Alpha particles have been use in ion chamber like fire alarms. When smoke from a fire picks up radioactive alpha particles, the electrical current in the device changed, triggering a fire alarm. Alpha particles used to treat some types of cancer as a tool for targeted therapy. Directing alpha particles to cancer cells can cause subtle damage to cancer cells without

significant damage to healthy tissue [93]. Alpha particles used in nuclear research to study atomic nuclei and nuclear structures. If you have a tiny, radioactive alpha particle, you can use it as a microscope to study nuclei and tiny particles and to understand the behavior of nuclei and nuclear reactions. Alpha particles used to determine concentrations of nuclear metals such as uranium and thorium in rock, soil, and mineral samples. This helps in exploring natural resources and geology [94, 95, and 96].

PART 4

METHODOLOGY

4.1. EXPERIMENTAL SETUP

4.1.1. Plasma System Preparation

High-purity argon 99.9N used as the discharge gas to create a cold plasma at atmospheric pressure. A quartz glass tube with a diameter of 4mm was preferred as the dielectric material in which the discharge took place. A capacitive coupled electrode designed in the plasma pen. The gas flow was set to 4l/min with the help of an analog scale and controlled flow meter. The plasma discharge initiated in the quartz tube by transferring a signal to the electrodes with the help of a high voltage low-frequency output power supply with controllable output power. As power, 8W transferred to the electrode system. The output voltage and frequency measured with a high-voltage probe connected to a digital handheld oscilloscope. The output voltage measured as 11.6kVpp and the frequency as 10 kHz. All of that shown in figures (4.1, 2, and 3).

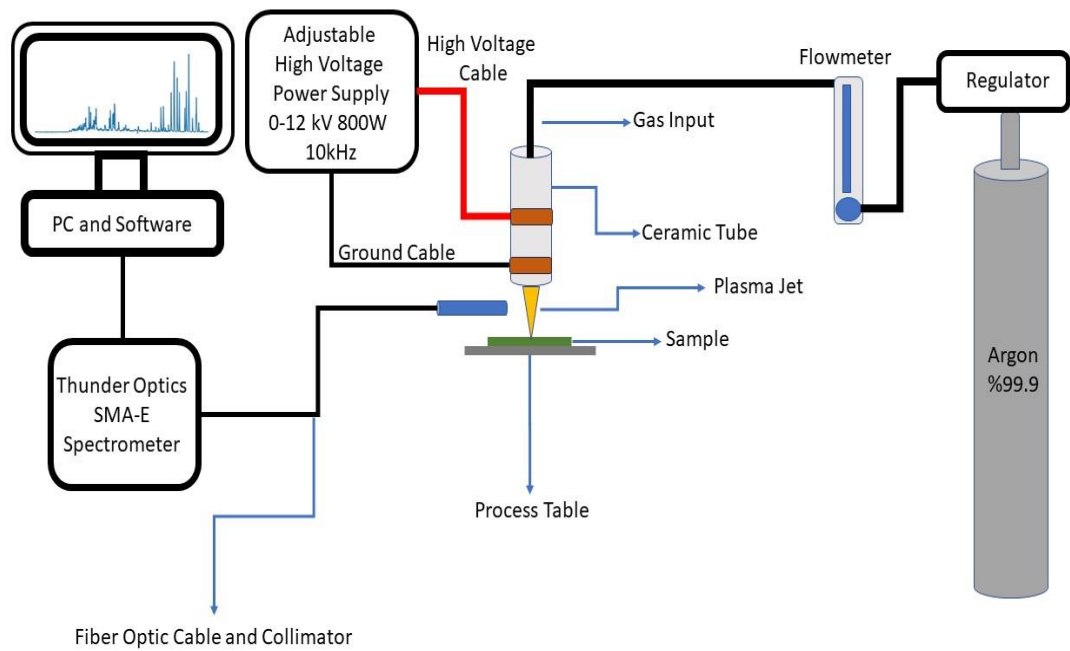


Figure 4.1. Atmospheric pressure cold plasma setup.

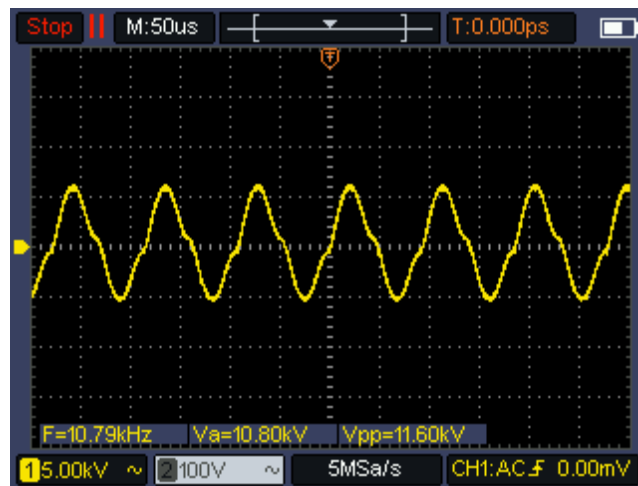


Figure 4.2. Observing the waveform of the output signal with the help of an oscilloscope.

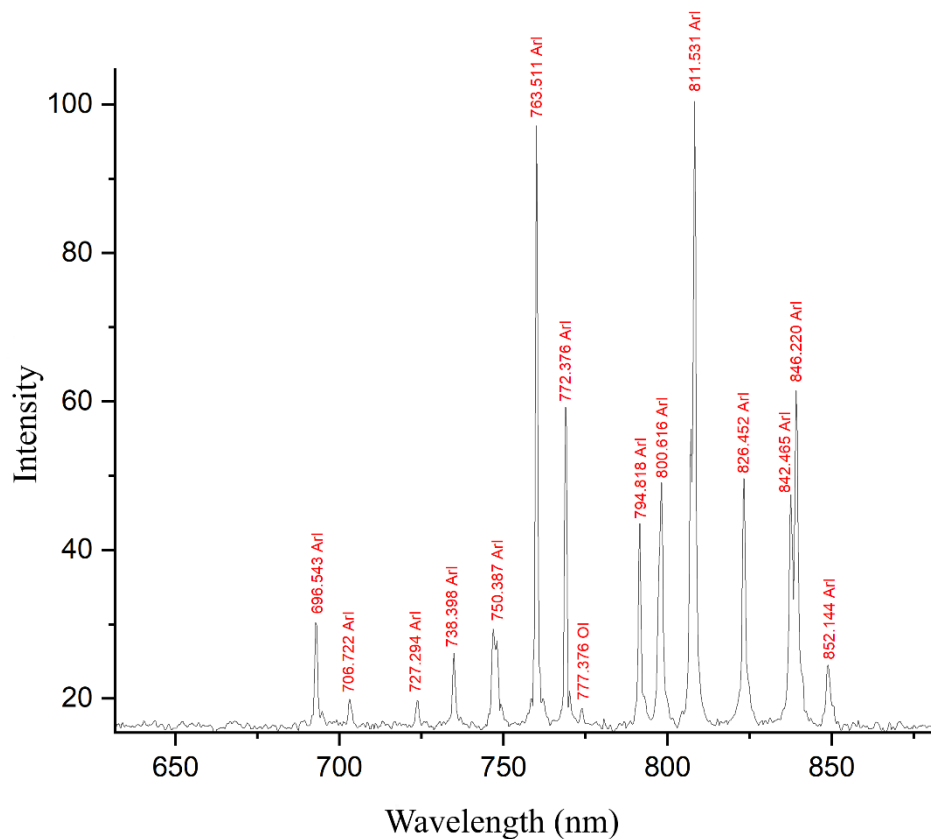


Figure 4.3. Argon cold plasma spectral lines.

4.1.2. Irradiation of CR-39 Detectors

In the Nuclear Physics Laboratory at the College of Science Ibn Al-Haitham, University of Baghdad, two groups G_1 and G_2 of solid-state nuclear track detectors CR-39 irradiated by alpha particles with an energy of (5,486 MeV) from the Americium (^{241}Am) with activity of ($5\mu\text{Ci}$) for group (1). Group (2) irradiated by Radium (^{226}Ra), with an activity of ($5\mu\text{Ci}$), which emits alpha particles with an energy of (4,871 MeV). Exposure time was 3 mints in contact with the sources.

4.1.3. Etching by Plasma

1. The irradiated detectors, as mentioned in paragraph (4.1.3), placed in front of the plasma flame to be etched at different distances (3, 5, 7, 9, 12) mm for the first group G_1 with different exposure times (5, 10, 20, 30, 40, 50, 60), and

the second group G2 (5, 10, 15, 20, 30, 40, 50) minutes. Figures (4. 4,5, and 6) showed these arrangements.

2. The detectors of groups G1 and G2 cleaned with distilled water and dried to transfer for the process of calculating the number of tracks per unit area.
3. An optical microscope (ANOVA) type (ZoomexXSP-44SM) with magnification (400X) used to observe and calculate the tracks in the detector CR-39 for groups G1 and G2 as shown in figure (4.8).
4. The temperatures generated on the surface by argon plasma were visualized with the help of Seek XR model thermal camera as shown in figure (4.9). After long-term application, surface temperatures measured as 43°C for argon plasma.
5. Recording the results by taking the average of ten attempts for each detector and then plotting the data for each area and etching method

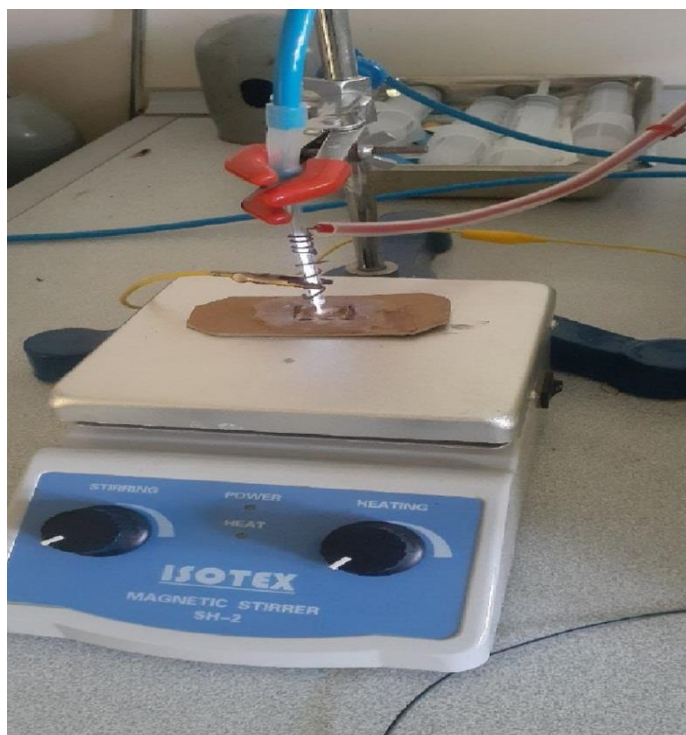


Figure 4.4. An image the base in which the detector was placed when etching



Figure 4.5. An image of the plasma system that was used.

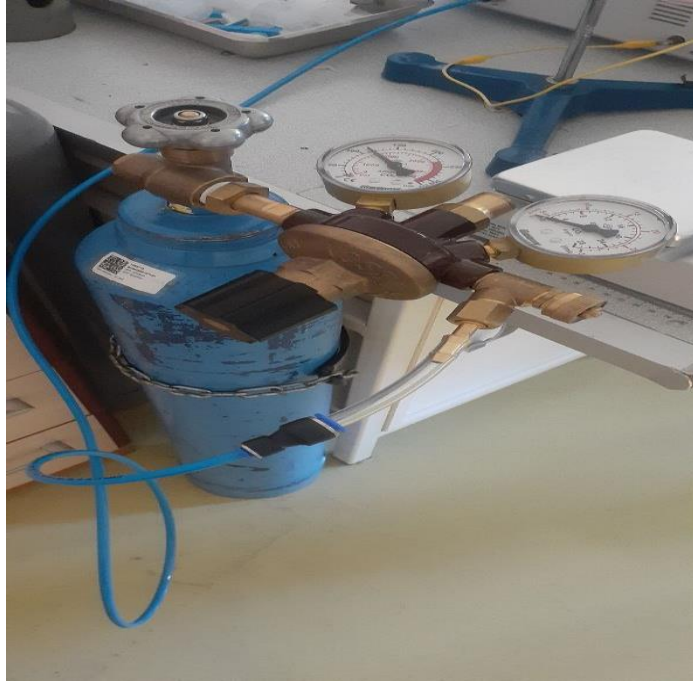


Figure 4.6. The argon bottle and meter used in the experiment.



Figure 4.7. An image of the power supply that was used.



Figure 4.8. Microscope used to detect antiquities.

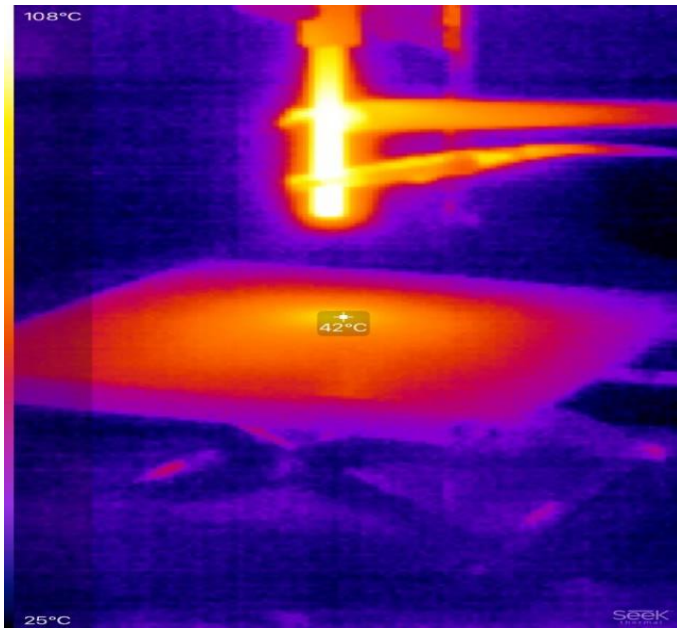


Figure 4.9. Argon a plasma thermal camera images.

4.2. RESULTS and DISCUSSION:

Tables 1 and 2 show the change in the number of alpha particle tracks in the CR-39 detector for the first group (G1), irradiated by a Americium-241 source with an activity of (1 μ ci), which emits alpha particles with an energy of 5.849 MeV, then etched with Argon plasma, as well as the second group, G2, irradiated by a radium-226 source with an activity of (10 μ ci), which emits alpha particles with an energy of 4,897MeV.

The tracks number recorded in Table (4.1 and 2) showed an increasing the number of tracks for the CR-39 detector with an increasing in the time period for G1 and G2, which recorded the highest values for track density of (4010.579, 3887.956, 3475.015, 3160.216, and 2691.835 track/mm²) at the time period of 40 minute for distances (3, 5, 7, 9, 12 mm) respectively. We also notice a decreasing in the highest values with increasing distance between the detector and the plasma source as shown in figures (4.10-14) for G1. This behavior was observed for the second group irradiated with the Radium-226 isotope, which appear in figures (4.28-32) of the results obtained for the values of the number of tracks for the periods (5, 10, 20, 30, 40, 50) minutes, as the highest count values appeared at the period 30 minutes, and that the highest count values decrease as the distance between the detector and the plasma source increases. The figures (4.15 and 16) represent the photos of tracks in CR-39 detectors for G1 etched by plasma, and figure (4.16d) etched by chemical solution. The figures (4.33 and 34) represent the photos of tracks in CR-39 detectors for G2 etched by plasma, and figure (4.34d) etched by chemical solution.

This behavior is consistent with the results obtained by Hamid et.al [15], because it differs from this work regarding the maximum count period was (20) minutes. Also, the fact that the Hamid source used cold helium plasma under plasma conditions differs from this work (we use Argon gas). In this work, the correlation coefficient was found for the count values recorded in the CR-39 detector with the count values recorded using cold plasma shown in figures (4.17-21) for G1 and figures (35-39) for G2. The correlation coefficient was strong for most periods and distances and was more than 0.60, which mean the result are more accurate. From observing all the

results and the similarity of the behavior in the cold plasma etching process. The process of matching was performed by fitting all the data, so it was in the form of a polynomial with fifth degree for most graphs, and including the fourth degree. This confirms one behavior and one response by the detector towards two different sources, and Argon cold plasma. All data shown in figures (4.22-26) for G1 and figures (4.40-44) for G2. And from Figure (4.27 and 4.45) for the values of counting tracks with distance (3,5, and 7) mm for time periods (5,10,20,30,40,50, and 60) minutes for G1 and G2, we find the relationship is inverse for each time period with the effect of plasma with increasing distance.

The values of the diameter of the track with the exposure time for each of the plasmas shown in Table (4.3) for G1 and G2. When drawing the relationship of the diameter of the track with the etching time. We notice that the diameter of the track increases with the exposure time to the plasma at the same distance of (3 mm) increases. Where its maximum value reaches at an exposure time of (40 minute), then the diameter of the tracks begins to decrease with increase the exposure time for argon and helium at a fixed distance of (3mm) as shown in figures (4.46 and 4.47).

Table 4.1. Track density with time at different distances for Argon gas G1.

Time (min)	Track density (tracks/mm ²)				
	D=3mm	D=5mm	D=7mm	D=9mm	D=12mm
5	1864.721	1213.021	1037.856	988.961	826.756
10	2140.275	1635.579	1358.26	1128.156	915.538
20	2961.646	2190.676	1772.579	1435.887	1120.164
30	3516.183	2994.042	2650.493	2169.52	1883.766
40	4010.579	3887.956	3475.015	3106.934	2691.835
50	3520.117	2793.234	2604.82	2036.216	1745.034
60	2993.428	2586.816	2217.954	1892.766	1563.883

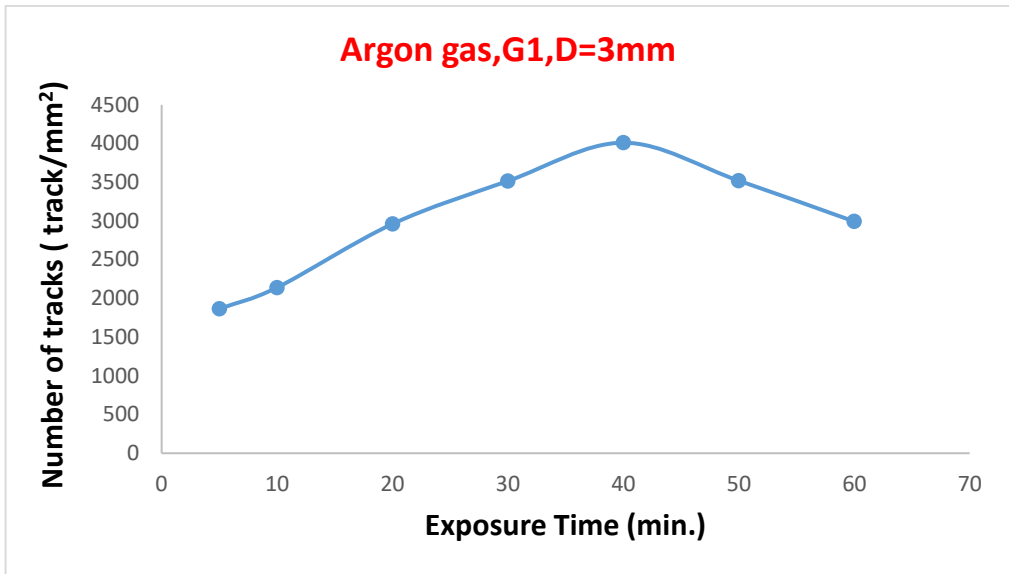


Figure 4.10. The track density with exposure time for a distance of (3) mm.

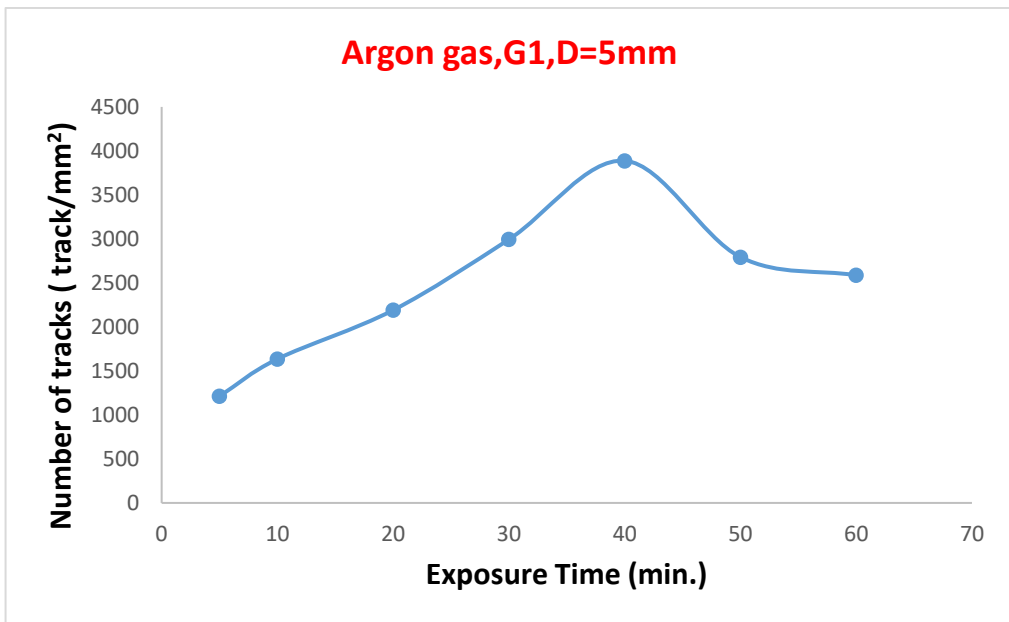


Figure 4.11. The track density with exposure time for a distance of (5) mm.

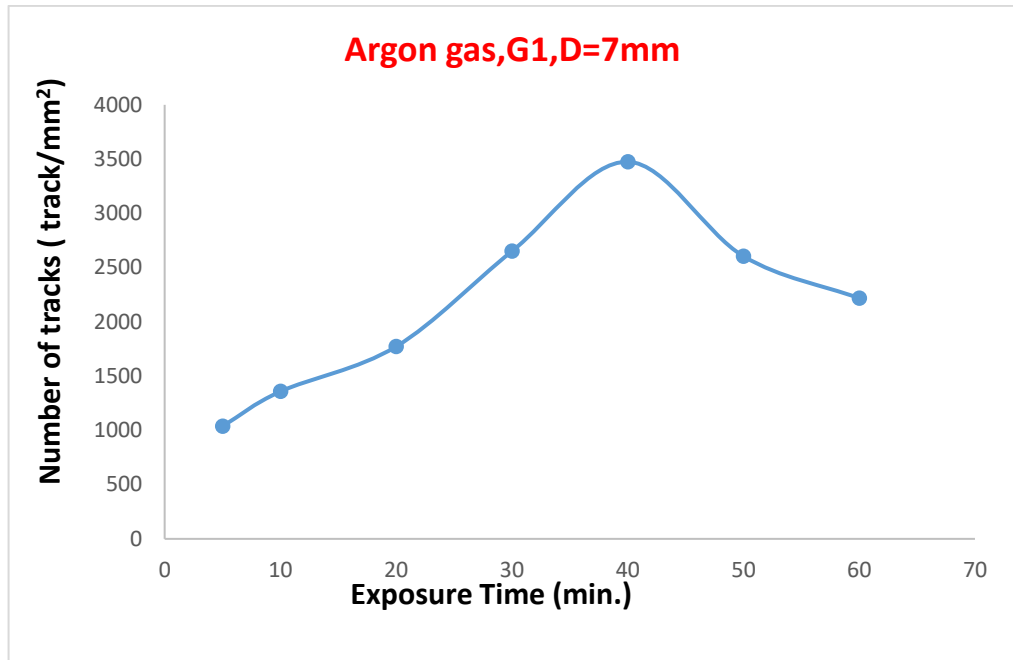


Figure 4.12. The track density with exposure time for a distance of (7) mm.

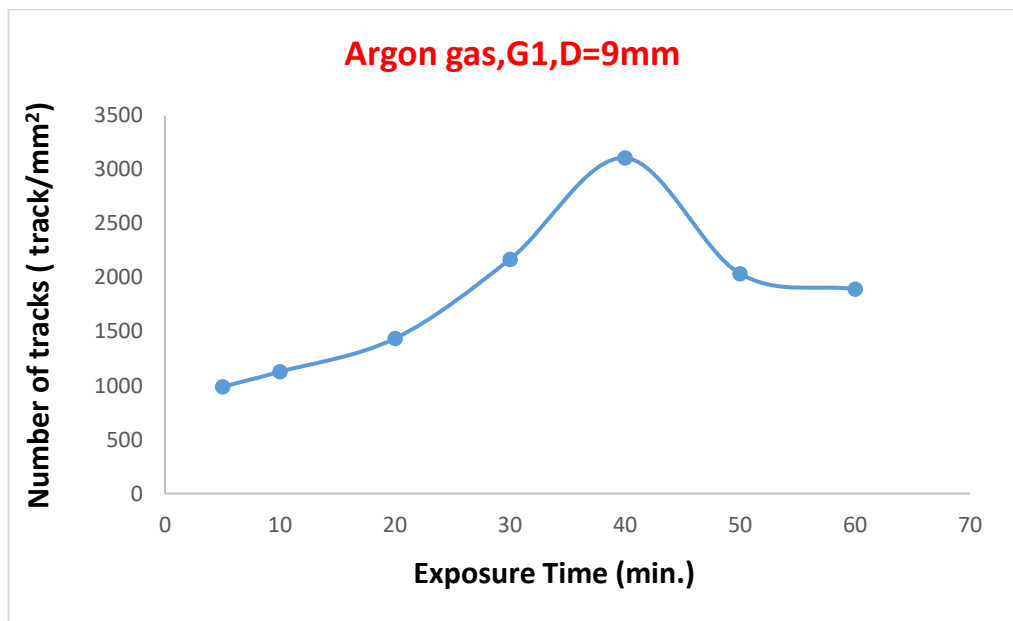


Figure 4.13. The track density with exposure time for a distance of (9) mm.

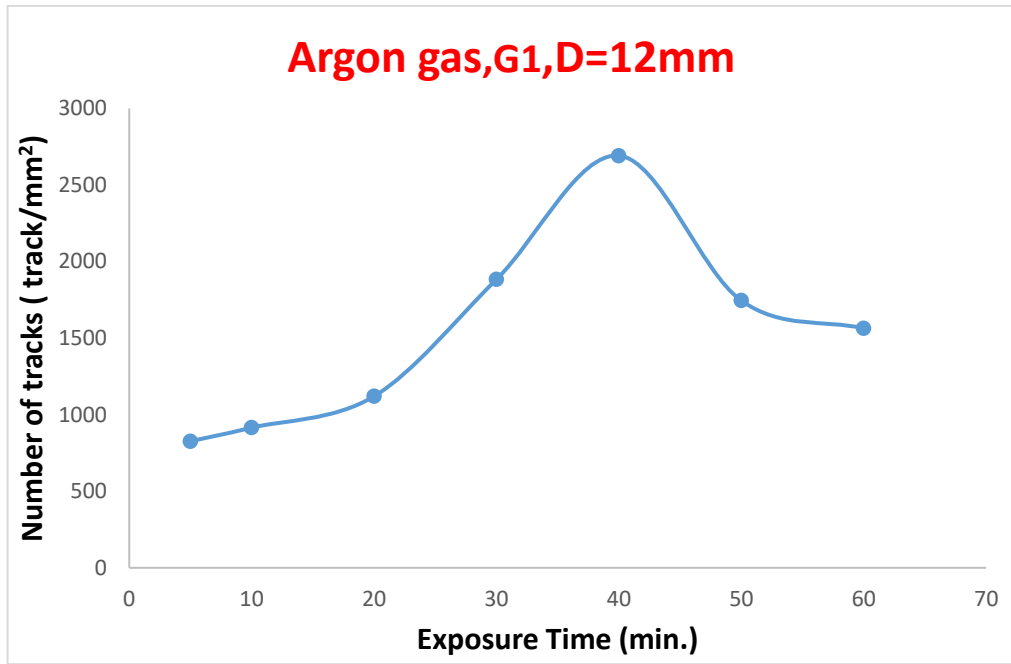


Figure 4.14. The track density with exposure time for a distance of (12) mm.

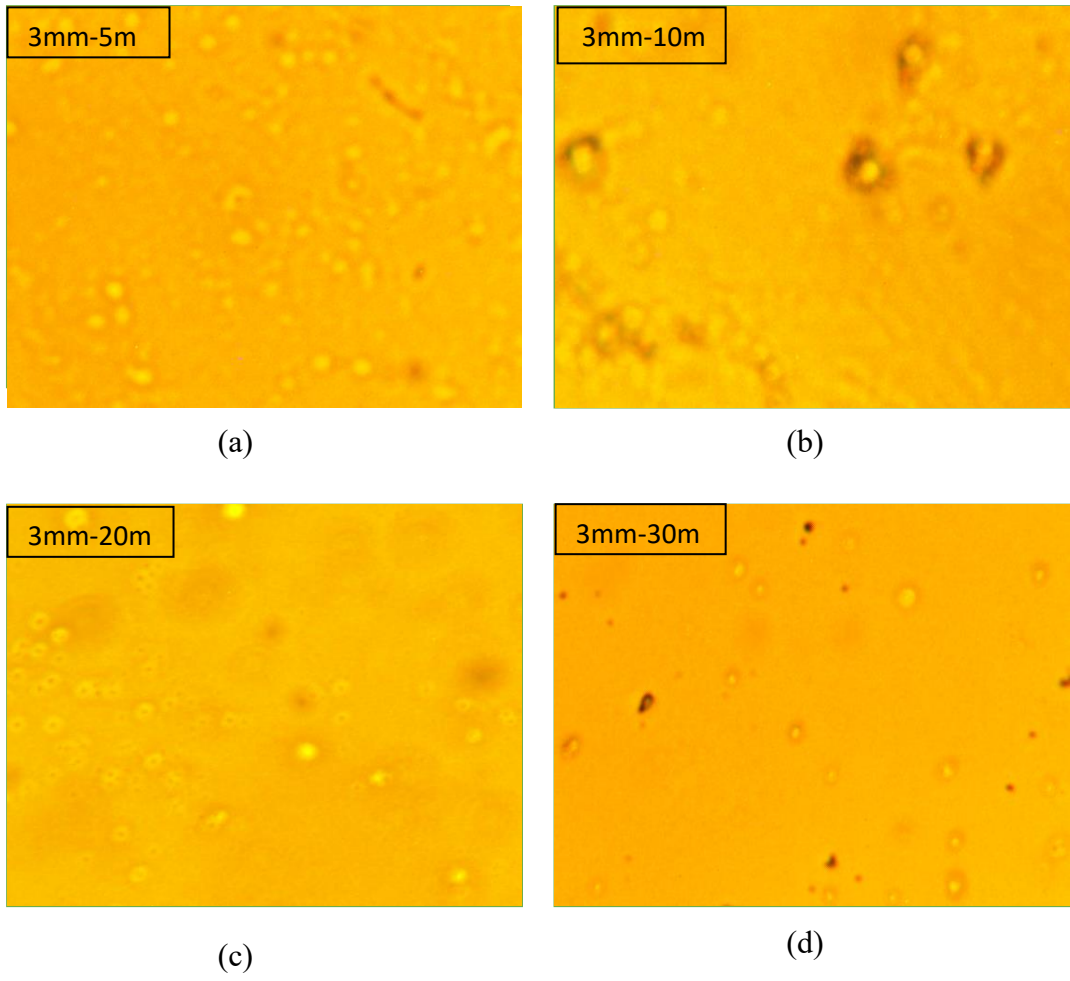


Figure 4.15. Etching effects for a distance of (3) mm and a time (a) 5 minutes (b) 10 minutes (c) 20 minutes (d) 30 minutes.

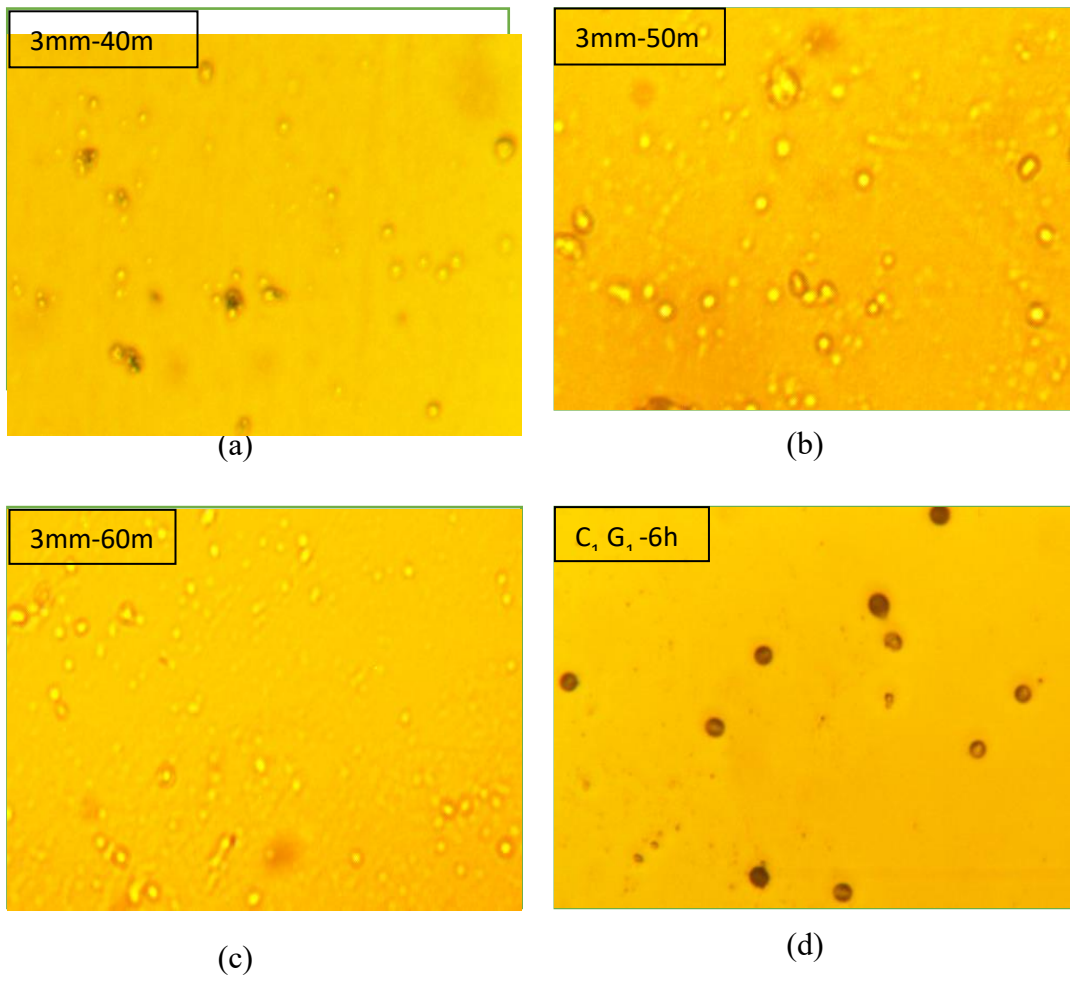


Figure 4.16. Etching effects for a distance of (3) mm with a time (a) 40 minutes (b) 50 minutes (c) 60 minutes and (d) for chemical etching (6 hours) .

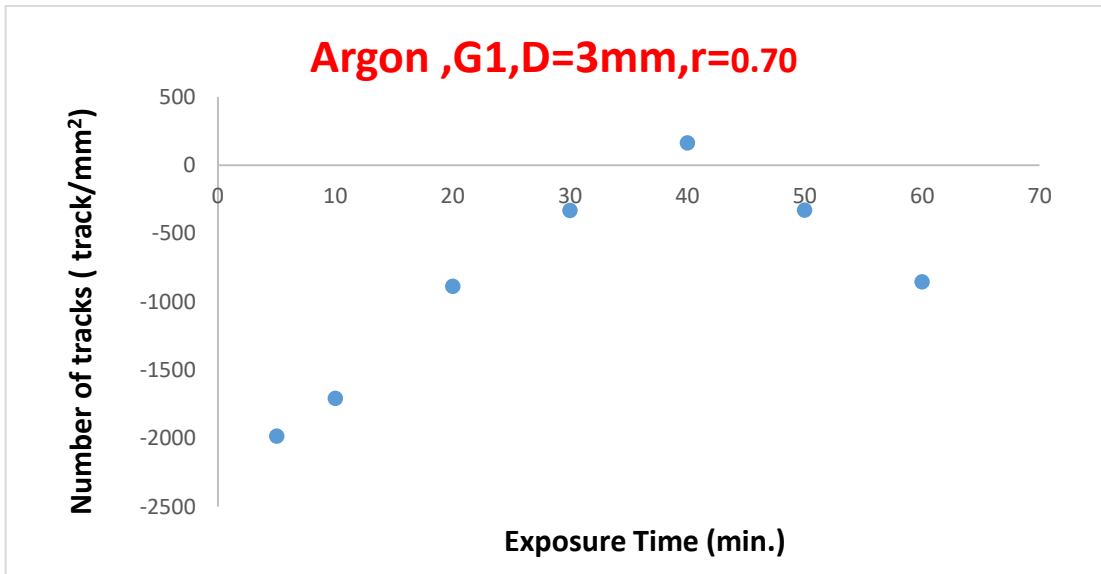


Figure 4.17. The correlation between results of chemical and plasma etching technique for Argon at D=3mm.

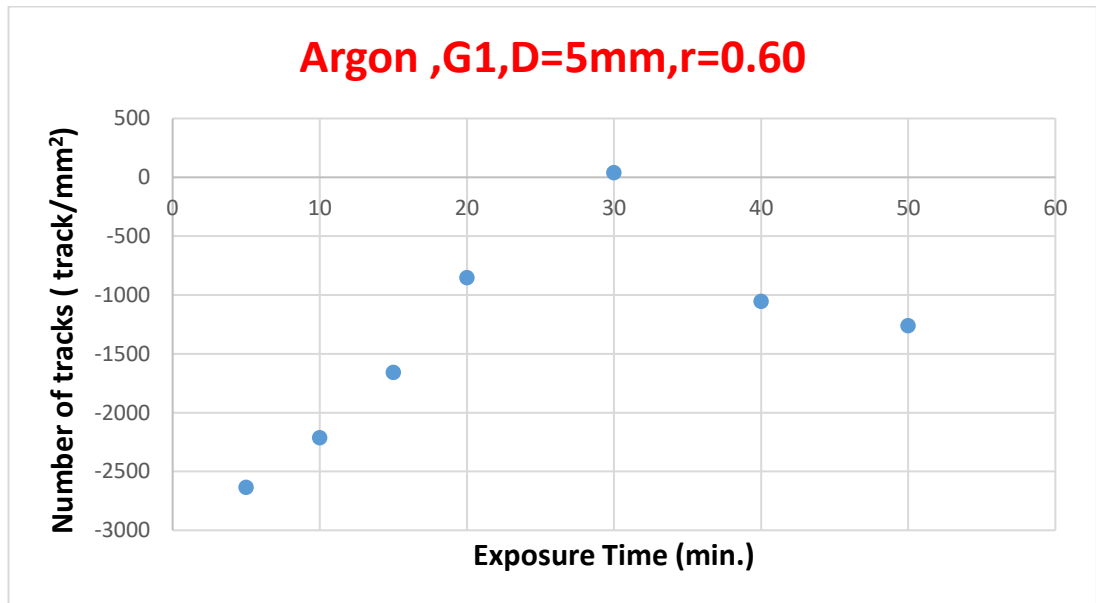


Figure 4.18. The correlation between results of chemical and plasma etching technique for Argon at D=5mm.

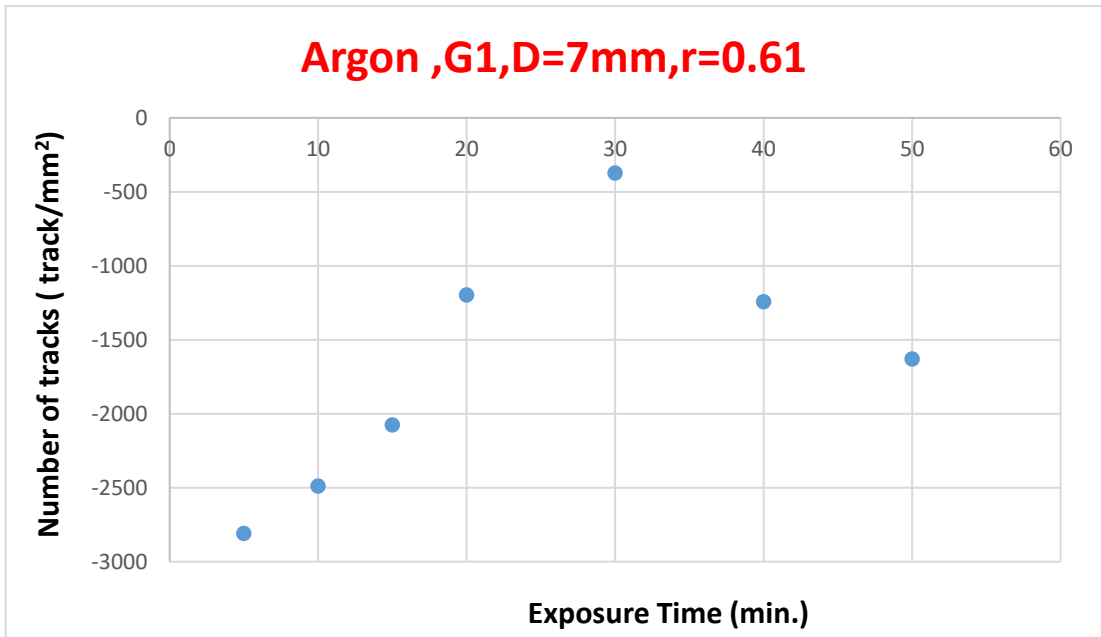


Figure 4.19. The correlation between results of chemical and plasma etching technique for Argon at D=7mm

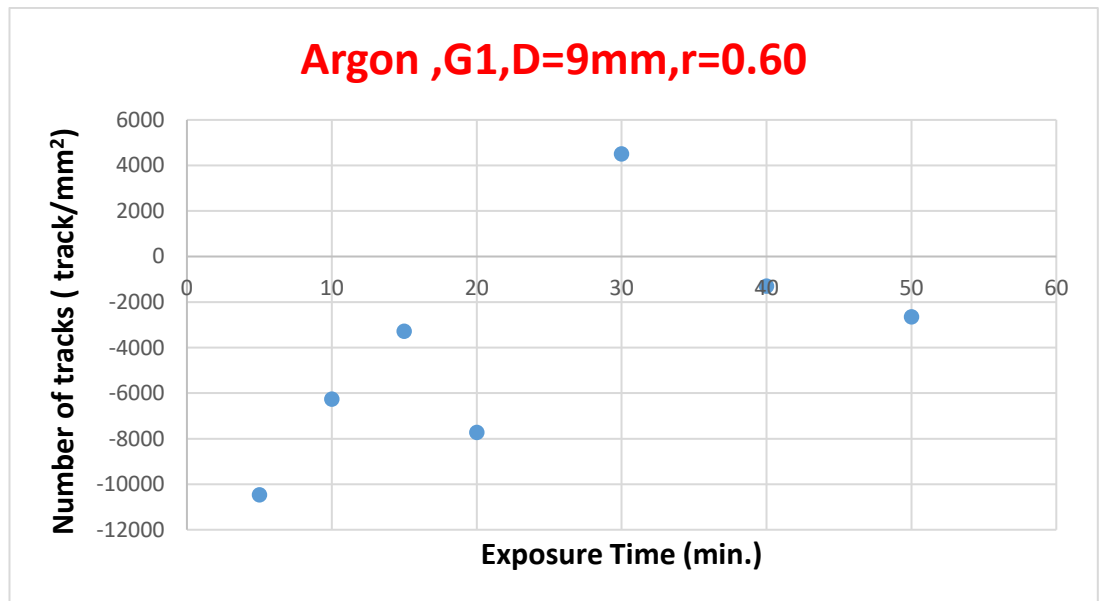


Figure 4.20. The correlation between results of chemical and plasma etching technique for Argon at D=9mm.

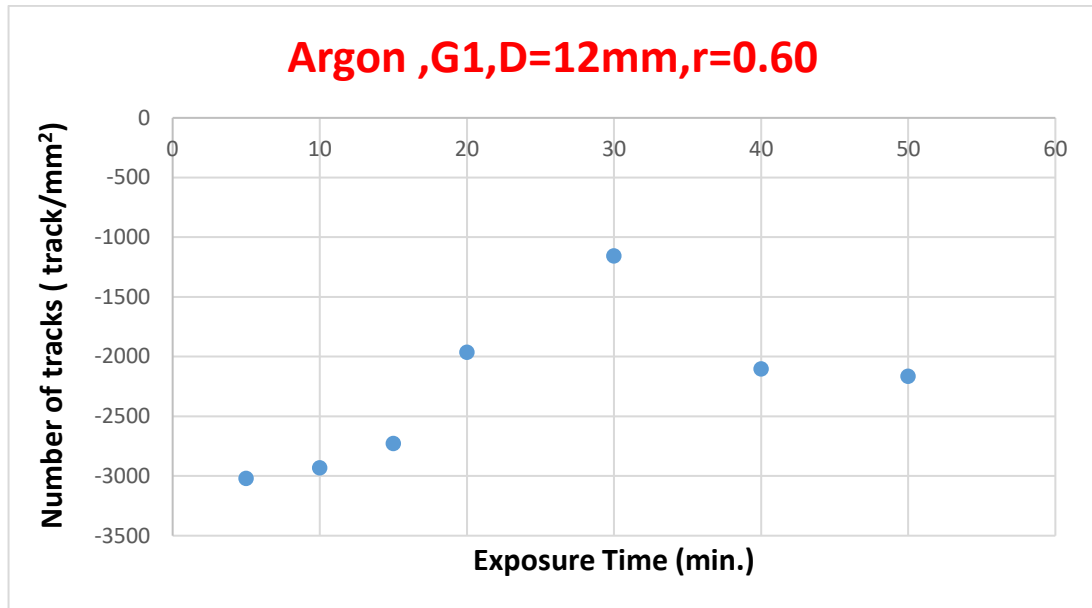


Figure 4.21. The correlation between results of chemical and plasma etching technique for Argon at D=12mm

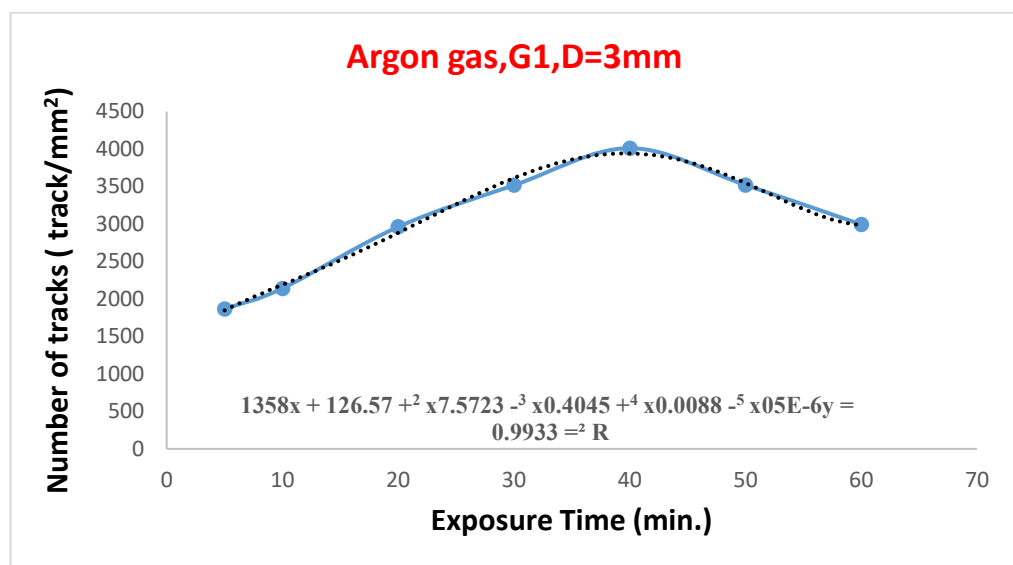


Figure 4.22. The fitting process for Argon gas at 3mm.

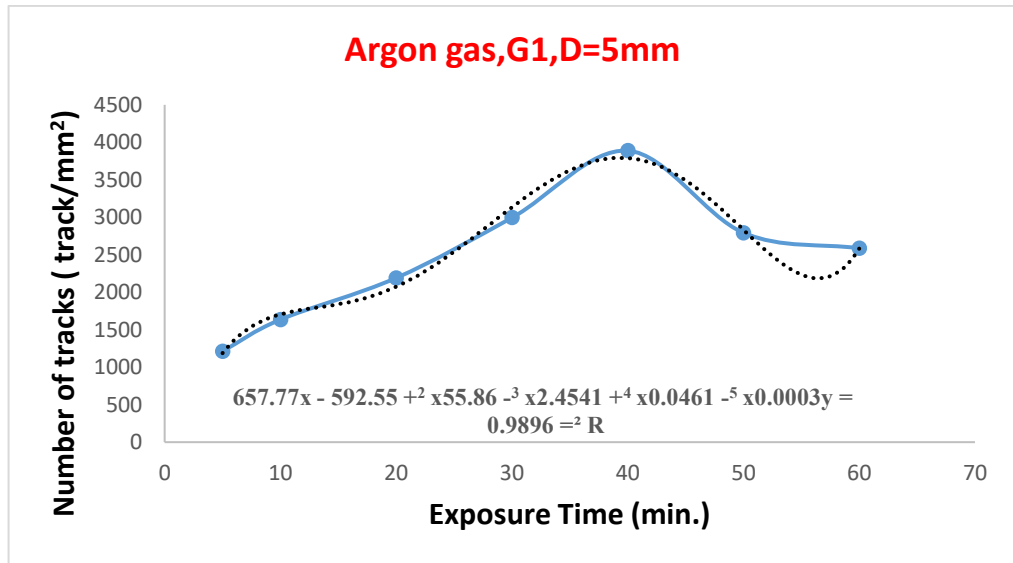


Figure 4.23. The fitting process for Argon gas at 5mm.

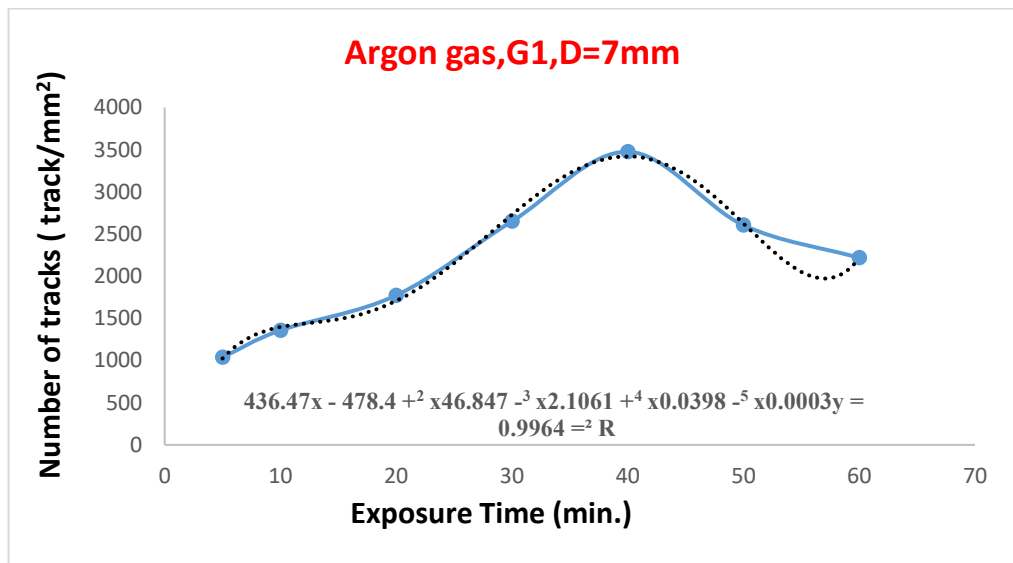


Figure 4.24. The fitting process for Argon gas at 7mm.

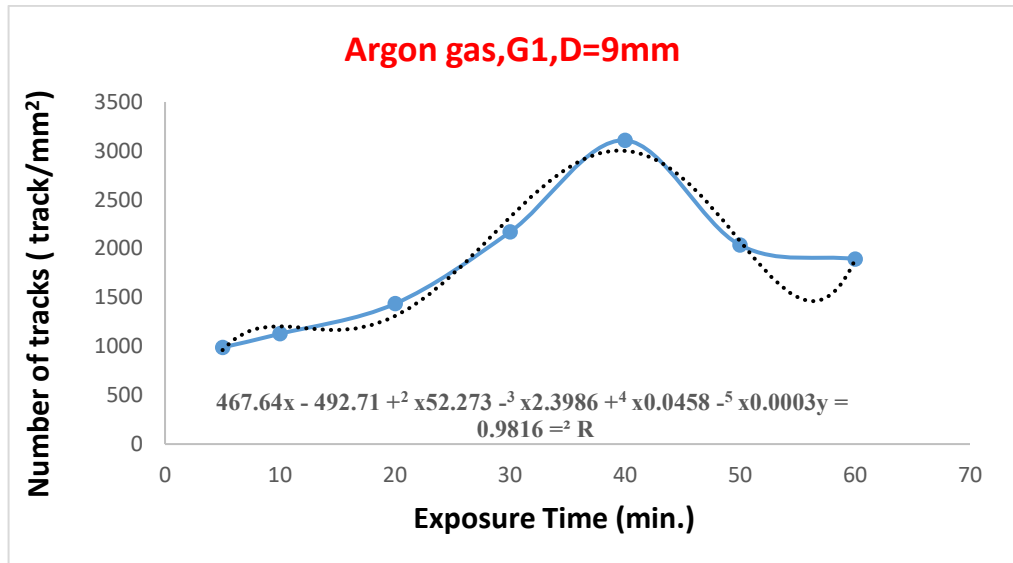


Figure 4.25. The fitting process for Argon gas at 9mm.

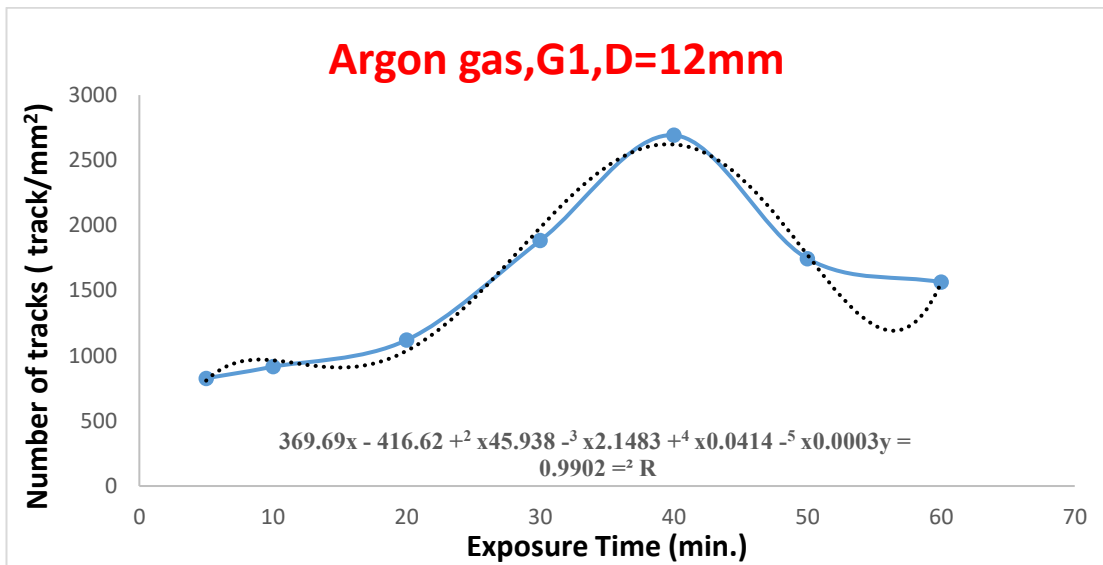


Figure 4.26. The fitting process for Argon gas at 12mm.

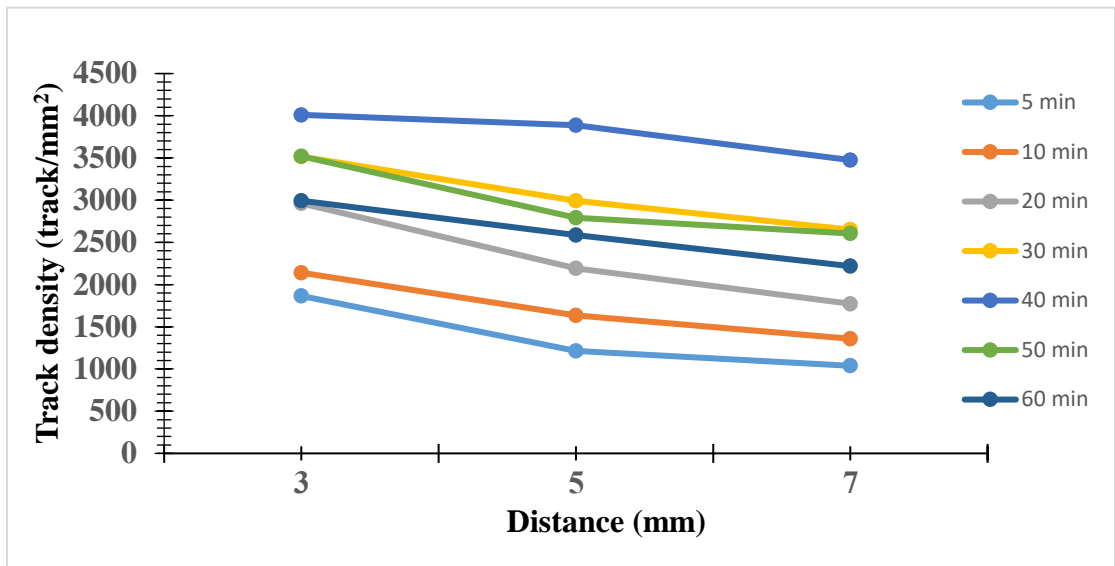


Figure 4.27. The relation between track density with distance at different time.

Table 4.2. Track density with time at different distances for Argon gas G2.

Time (min)	Track density (tracks/mm ²)				
	D=3mm	D=5mm	D=7mm	D=9mm	D=12mm
5	5917.16	5638.328	5168.523	4925.026	4117.245
10	10519.4	9840.297	6791.3	5753.596	4669.244
15	11670	12826.78	9040.153	7150.717	5735.24
20	16600.9	18382.64	13084.12	11086.25	9607.267
30	20896.4	20610.46	17340.33	15534.67	13432.26
40	18519.4	14808.02	13024.1	10140.36	8934.574
50	12722.1	13451.68	11333.75	9388.119	7788.137

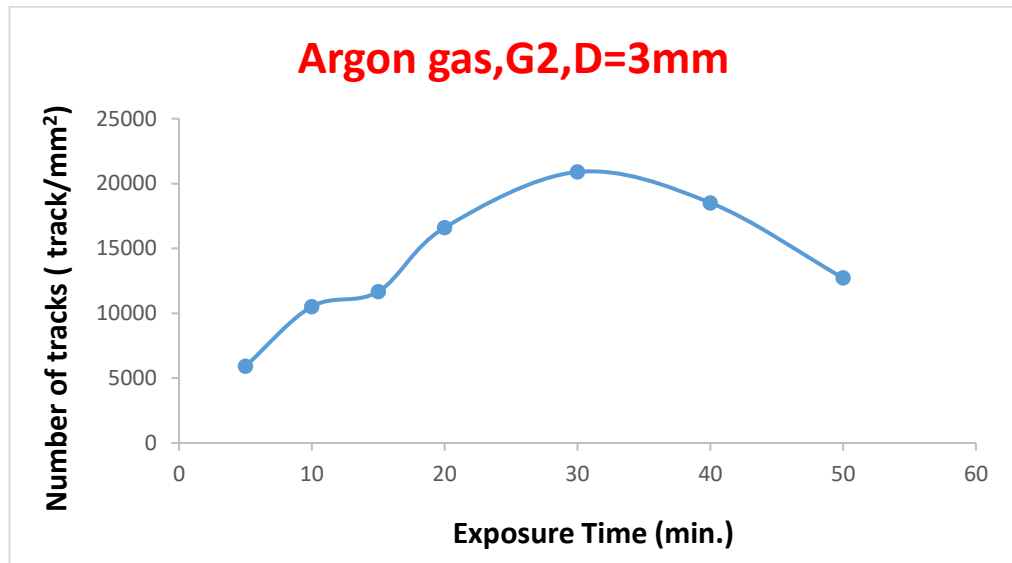


Figure 4.28. The track density with exposure time for a distance of (3) mm.

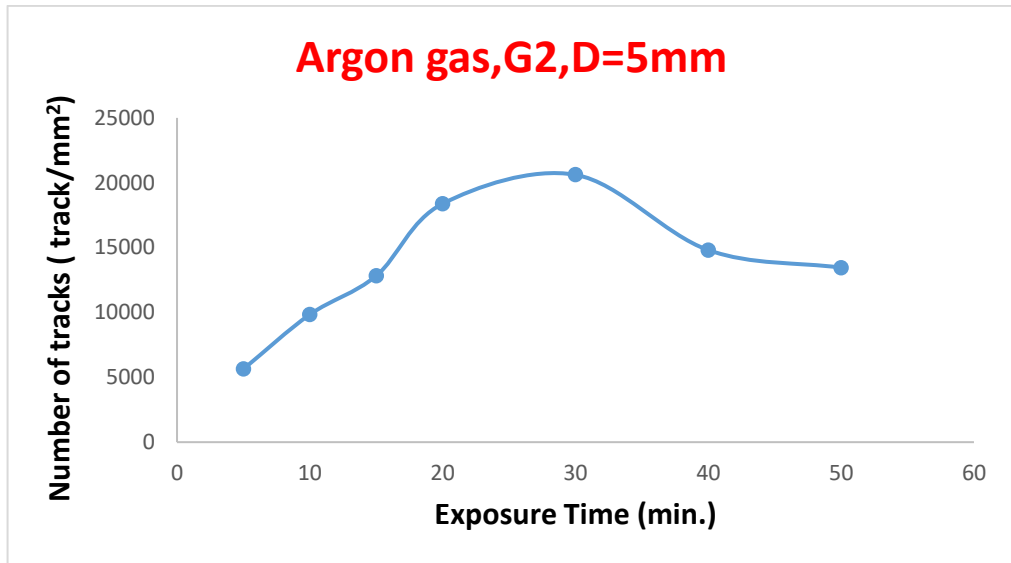


Figure 4.29. The track density with exposure time for a distance of (5) mm.

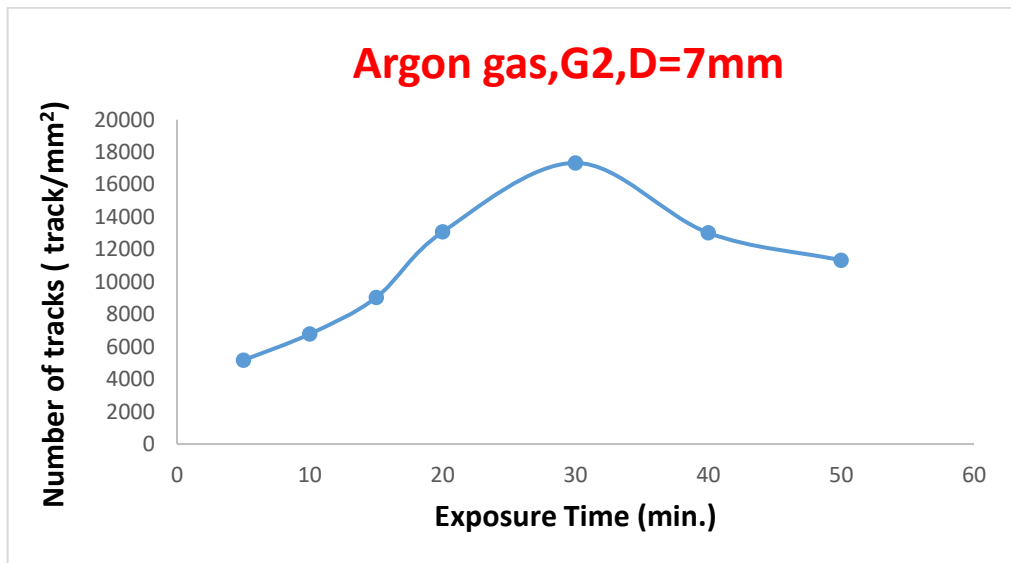


Figure 4.30. The track density with exposure time for a distance of (7) mm.

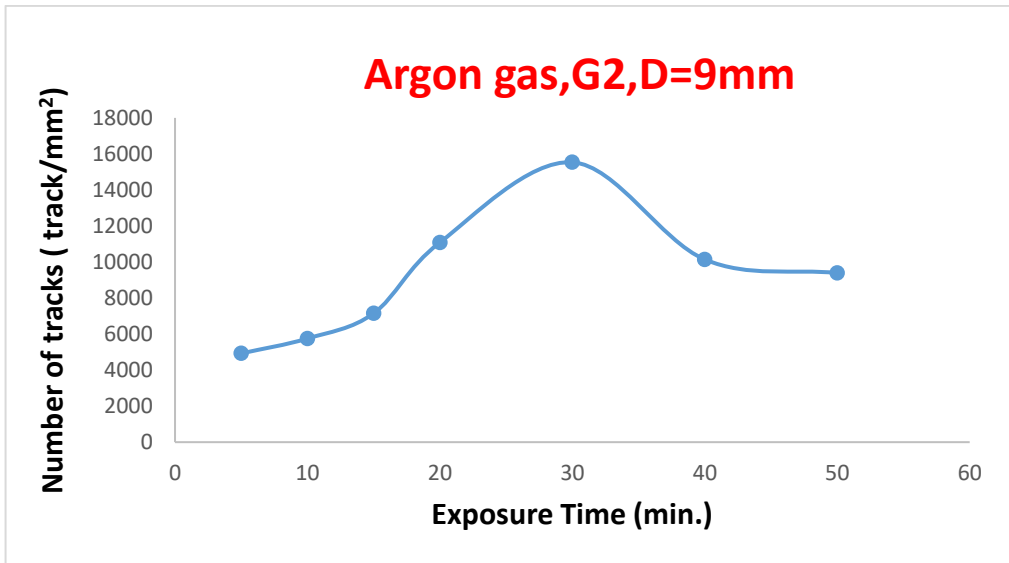


Figure 4.31. The track density with exposure time for a distance of (9) mm.

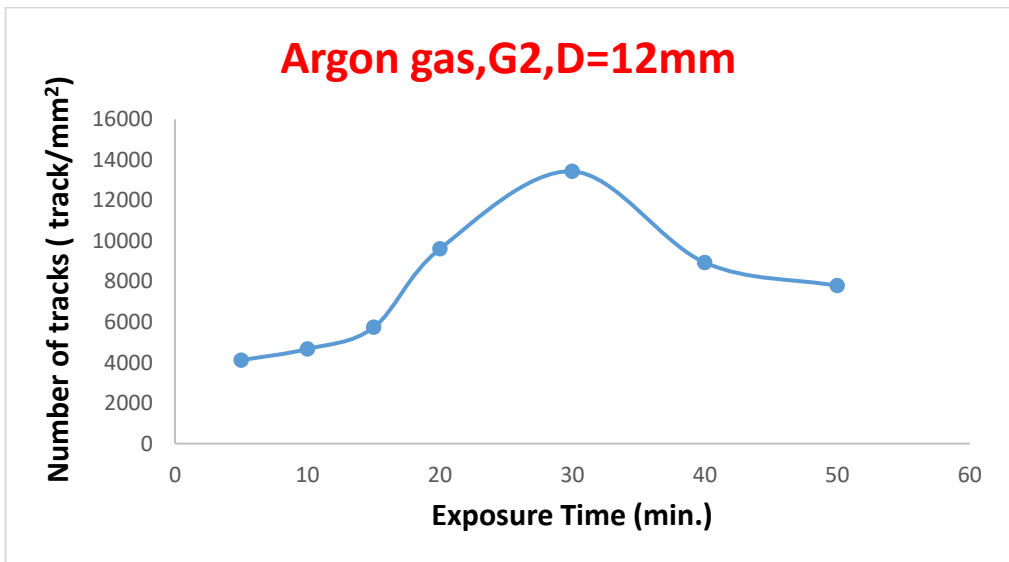


Figure 4.32. The track density with exposure time for a distance of (12) mm.

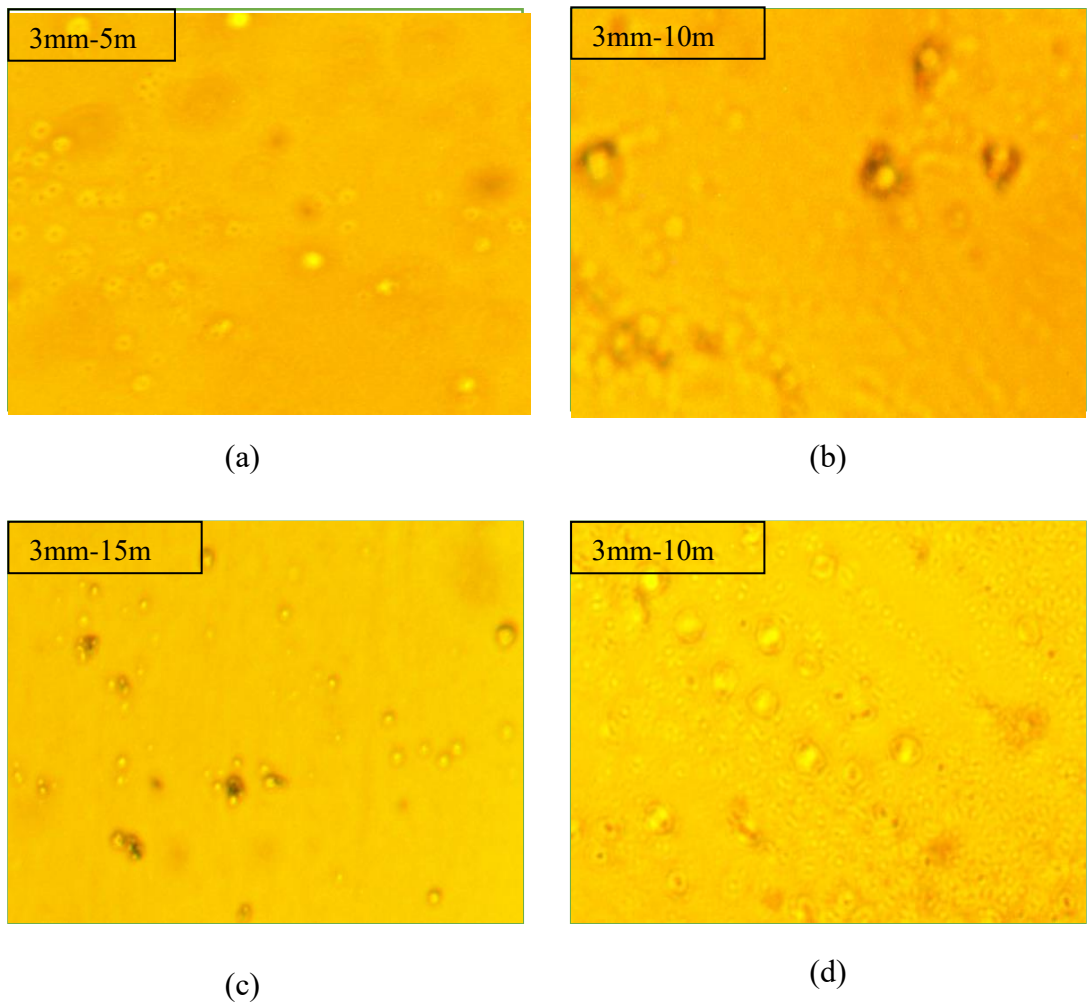


Figure 4.33. Etching effects for a distance of (3) mm and a time (a) 5 minutes (b) 10 minutes (c) 15 minutes (d) 20 minutes.

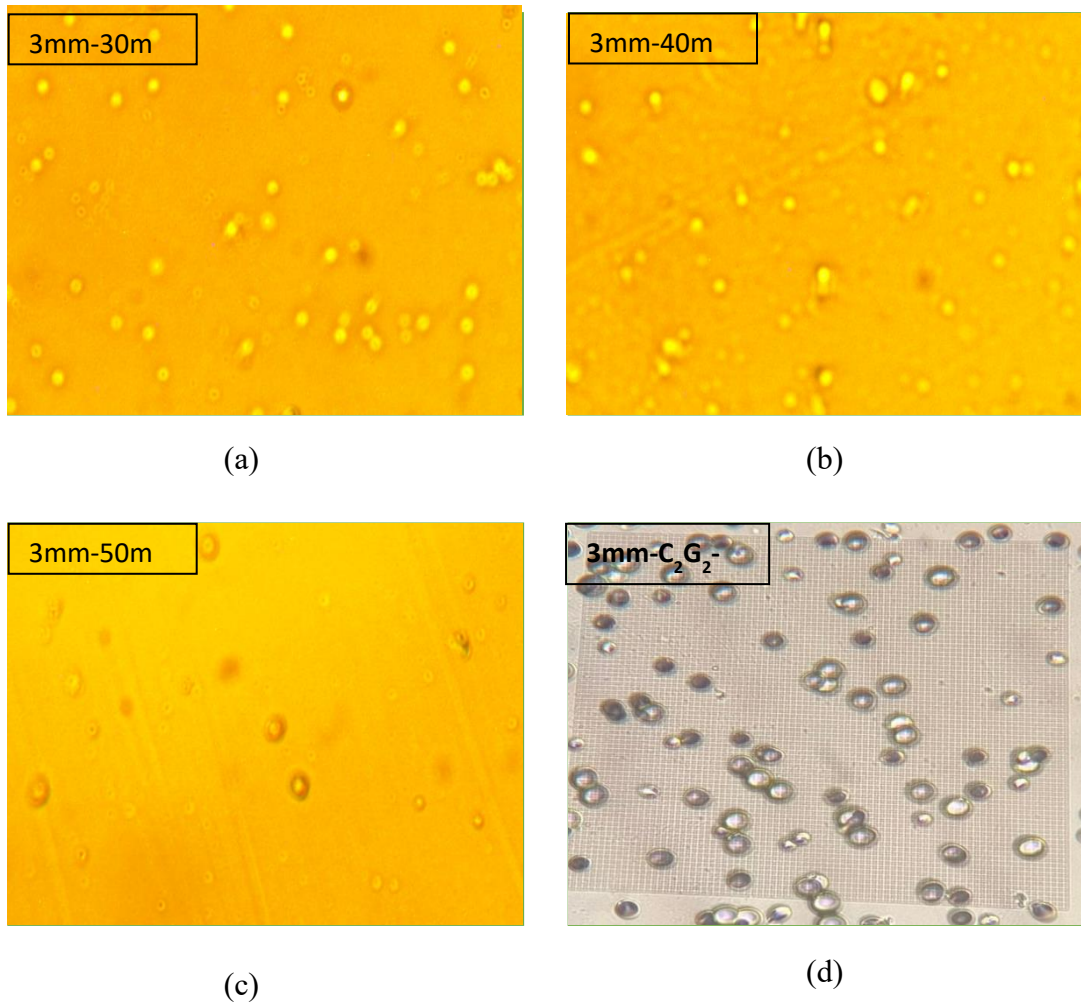


Figure 4.34. Etching effects for a distance of (3) mm with a time (a) 30 minutes (b) 40 minutes (c) 50 minutes and (d) for chemical etching (6 hours) .

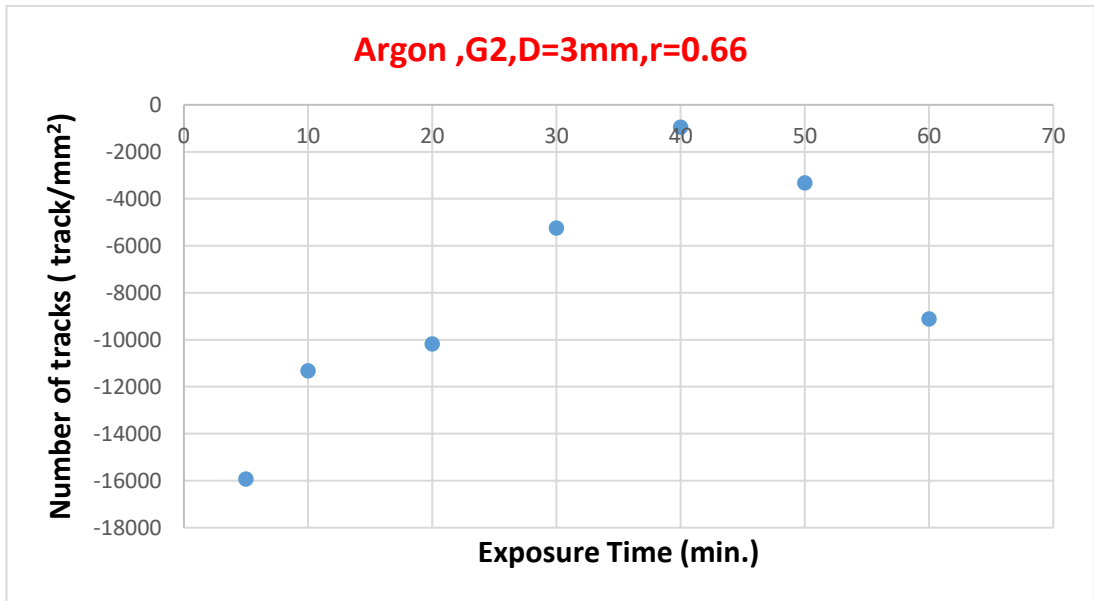


Figure 4.35. The correlation between results of chemical and plasma etching technique for Argon at D=3mm.

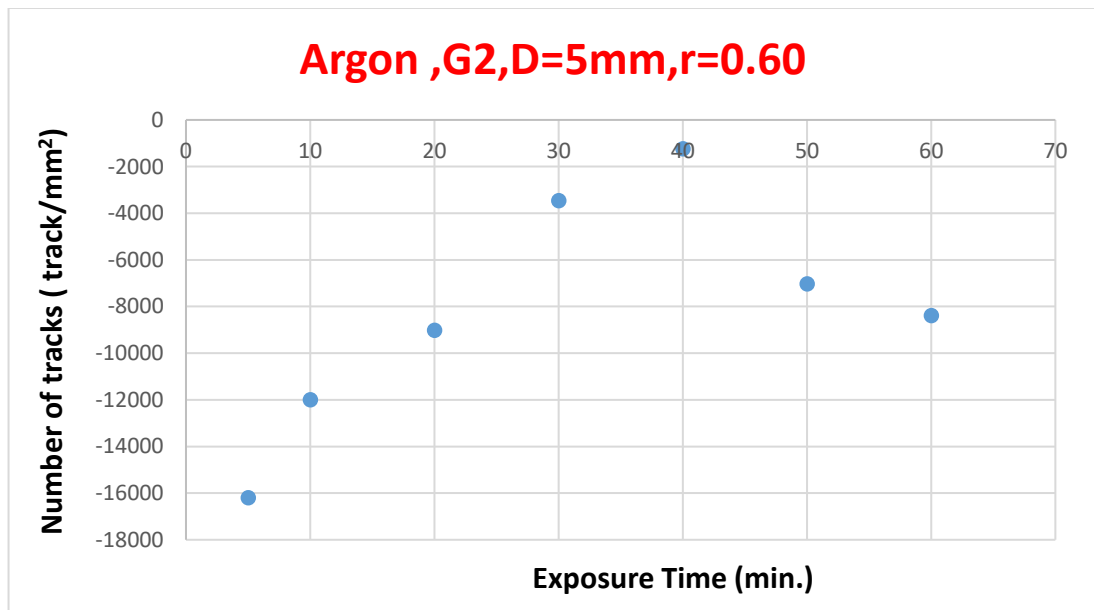


Figure 4.36. The correlation between results of chemical and plasma etching technique for Argon at D=5mm.

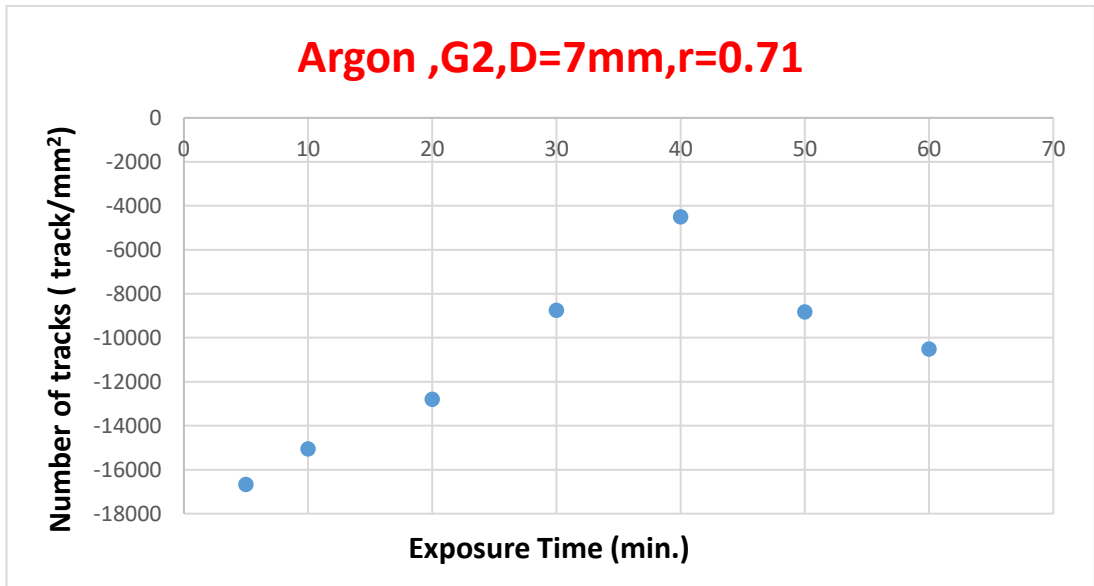


Figure 4.37. The correlation between results of chemical and plasma etching technique for Argon at D=7mm.

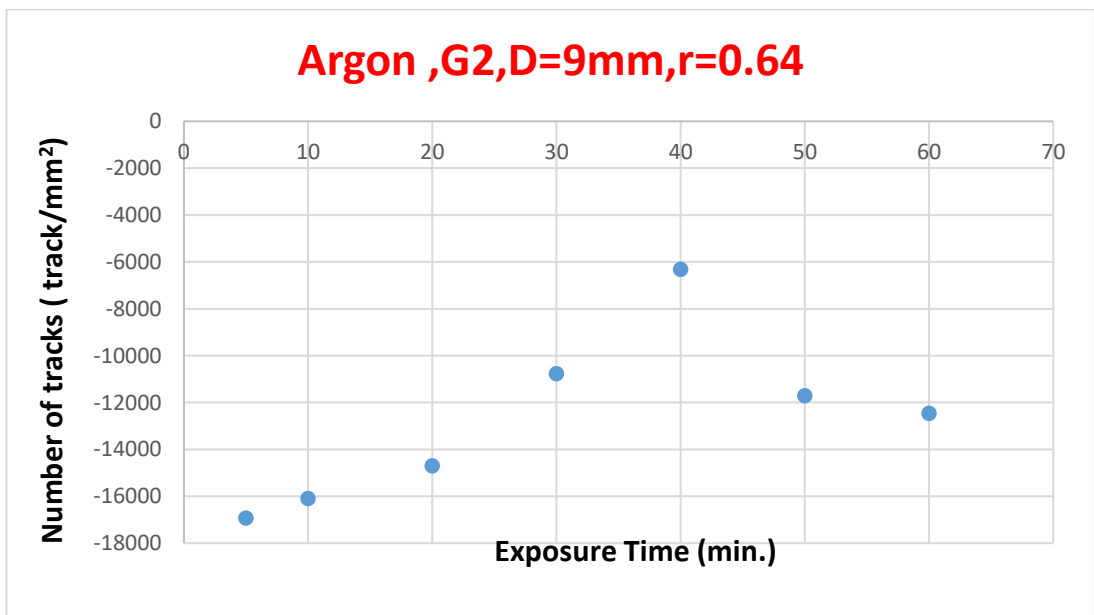


Figure 4.38. The correlation between results of chemical and plasma etching technique for Argon at D=9mm.

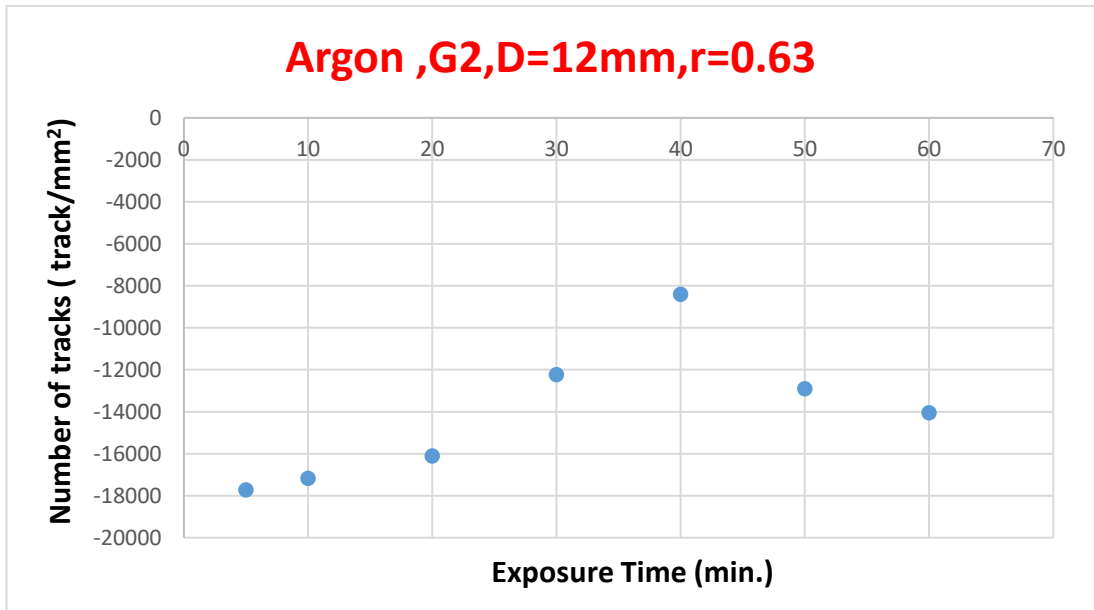


Figure 4.39 The correlation between results of chemical and plasma etching technique for Argon at D=12mm.

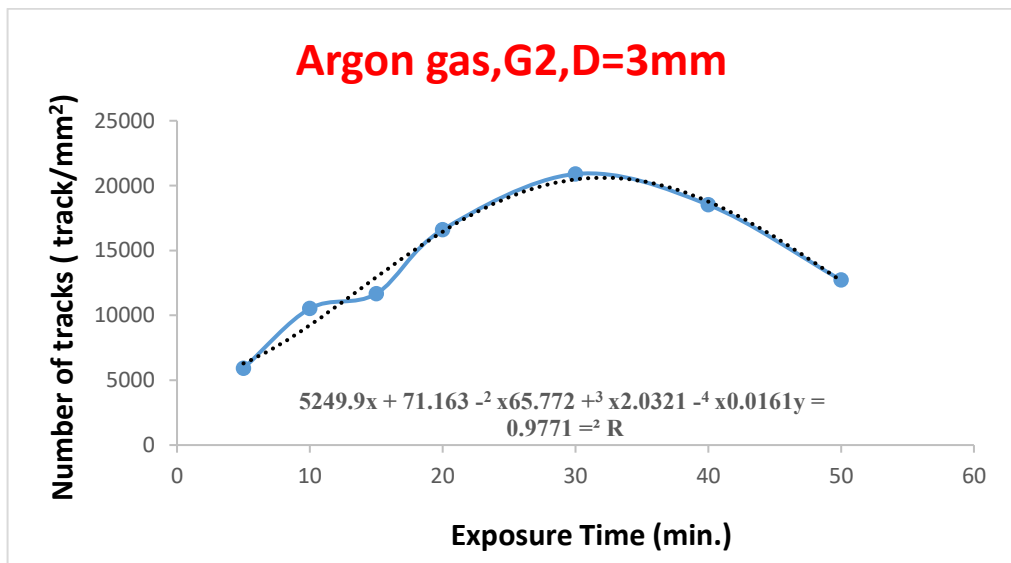


Figure 4.40. The fitting process for Argon gas at 3mm.

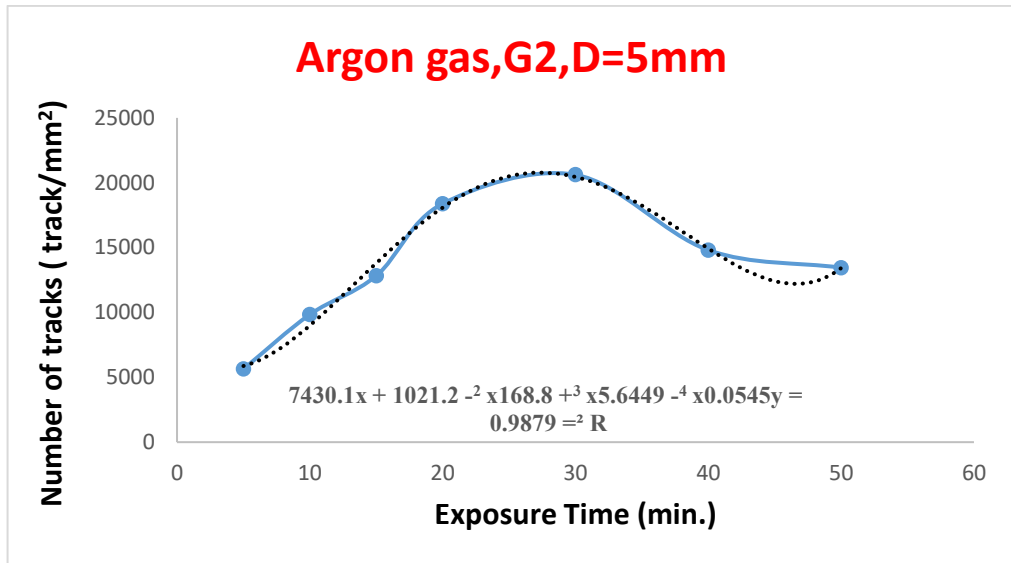


Figure 4.41. The fitting process for Argon gas at 5mm.

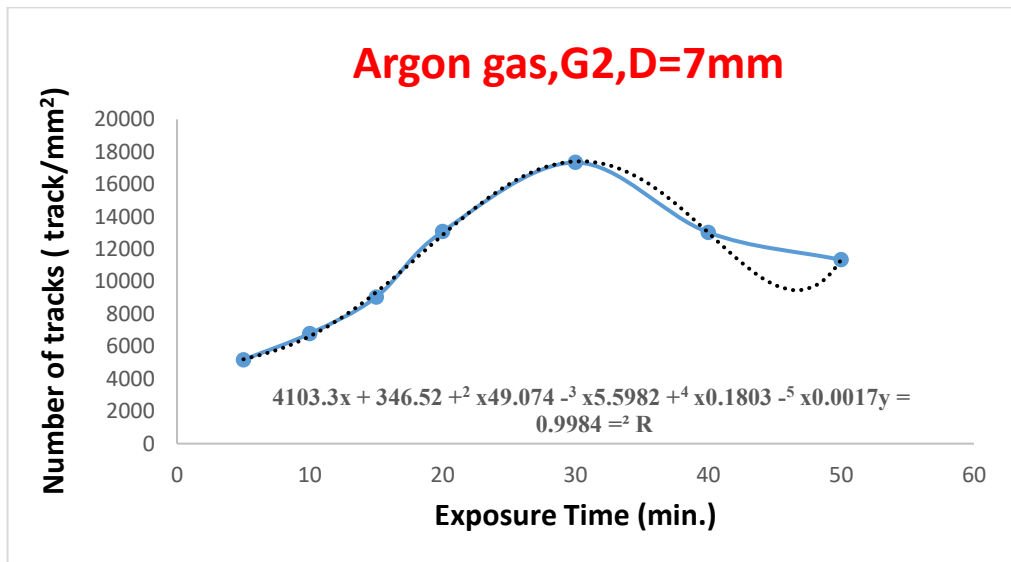


Figure 4.42. The fitting process for Argon gas at 7mm.

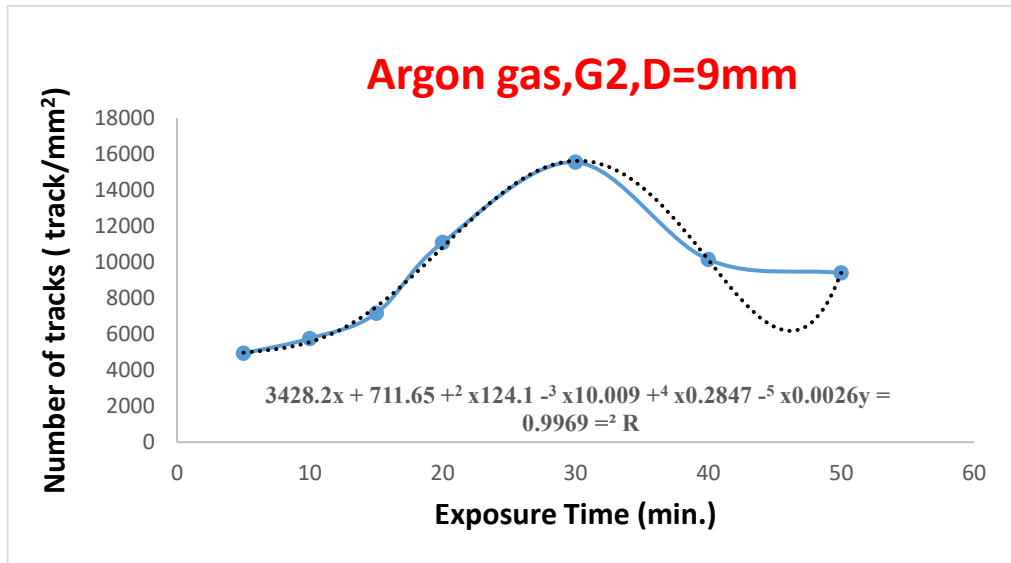


Figure 4.43. The fitting process for Argon gas at 9mm.

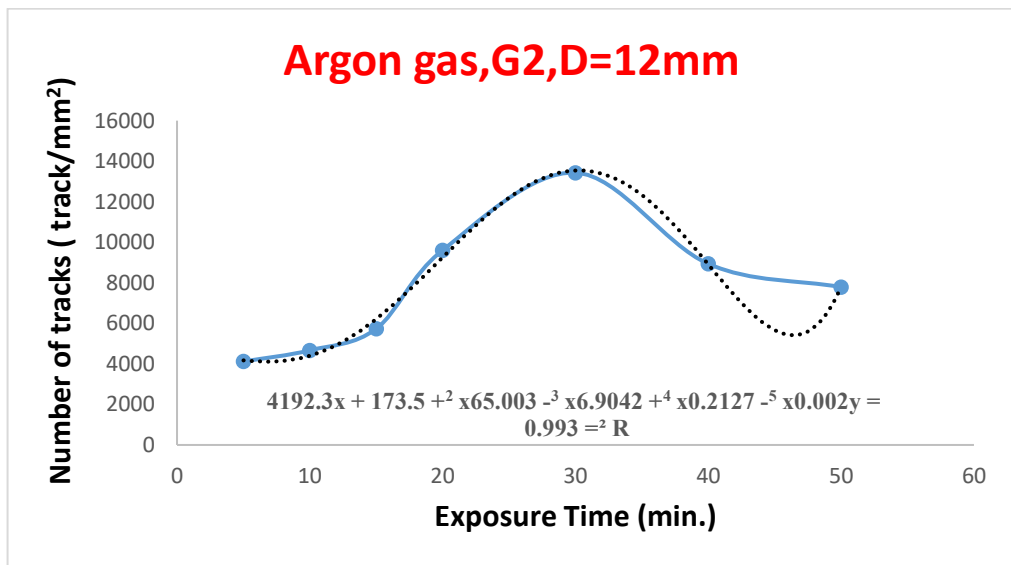


Figure 4.44. The fitting process for Argon gas at 12mm.

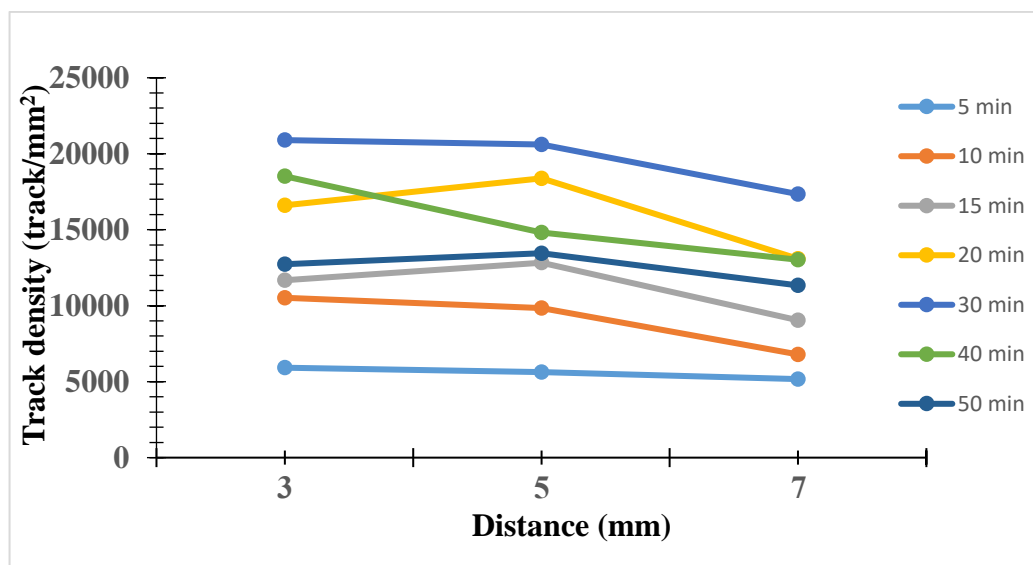


Figure 4.45. Change of track detectors according to the relationship between time and distance.

Table 4.3. The diameter of the track with the exposure time for each of the plasma.

Time (min)	Argon (3mm-G1) D(μm)	Argon (3mm-G2) D (μm)
0	0	0
5	9.7	9.9
10	12	11.9
20	14.7	14.5
30	18.3	18.4
40	21.0	20.9
50	17.9	18.0
60	16.2	16.4

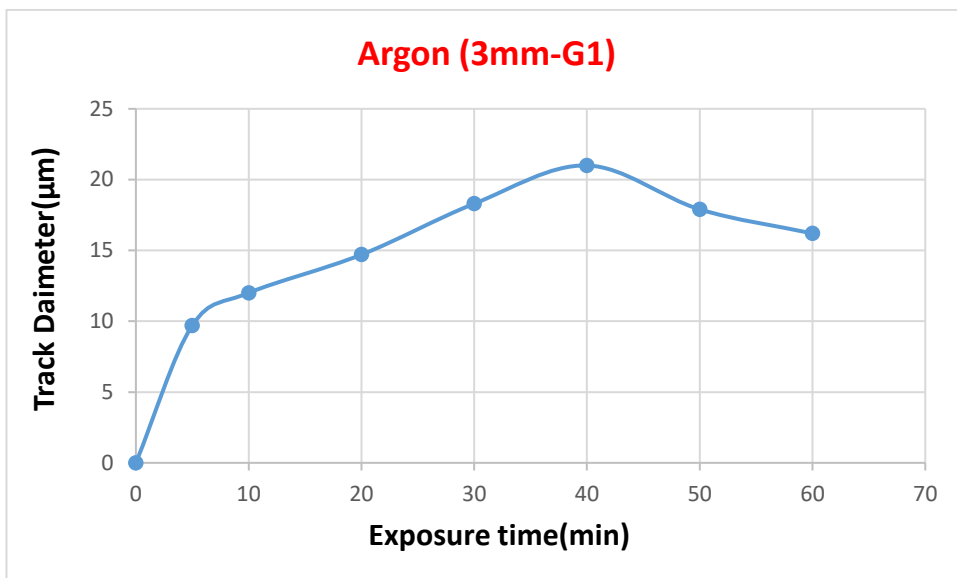


Figure 4.46. The diameter of the track with the exposure time for Argon gas at 3mm-G1.

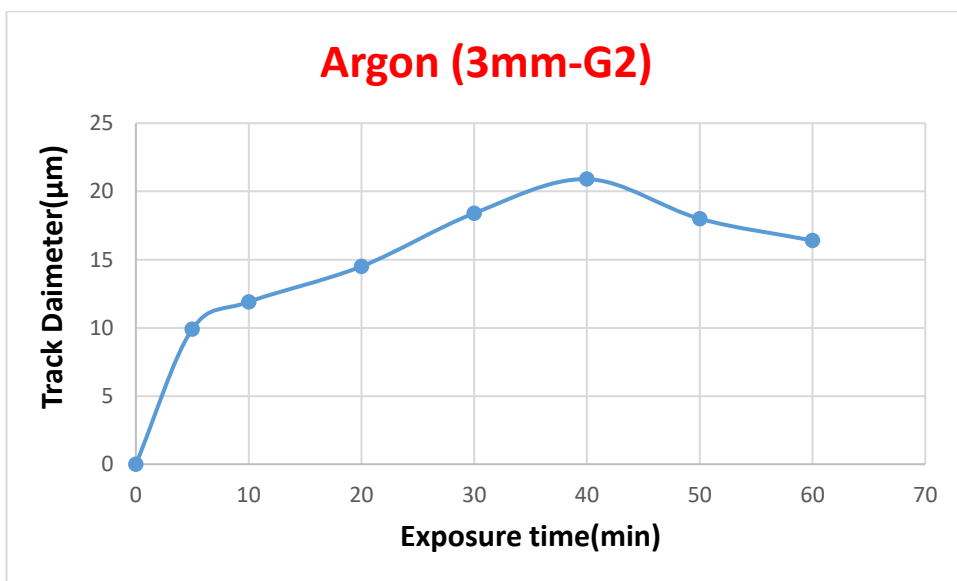


Figure 4.47. The diameter of the track with the exposure time for Argon gas at 3

PART 5

CONCLUSION

1. It is possible to adopt the method of etching the argon gas plasma for the alpha particles emitted by the isotope Am-241, with energy of 5.486MeV, with an activity of 1 μ Ci within the first group, and the alpha particles emitted from radium -226, with energy of 4.871MeV, with an activity of 10 μ Ci
2. Adopting the plasma etching method as an alternative to chemical etching by reducing the etching period from 6 -7 hours to 30 - 40 minutes, and by calculating the correlation coefficient for the number of tracks using plasma etching with the number of tracks in the chemical etching process.
3. It was found from the fitting process for all the graphical forms of the plasma etching process, that the equations represent a polynomial of the fourth degree for most of them and of the fifth degree for some of them. We can rely on these equations in choosing the appropriate conditions for the plasma etching process, especially since the graphical shapes and fittings indicate the same behavior of the process. Plasma etching for all periods and at different distances.
4. We conclude from the fitting process of calculating the correlation coefficient that the correlation coefficient decreases with increasing of distance between the plasma source and the detector.
5. The diameter of the track for the two groups (G1, and G2) increases with the exposure time to the plasma at the same distance of (3 mm) increases. Where its maximum value reaches at an exposure time of (40 minute), then the diameter of the tracks begins to decrease with time increases.

REFERENCES

1. Linet, M. S., Kim, K. P., Miller, D. L., Kleinerman, R. A., Simon, S. L., & de Gonzalez, A. B. (2010), Historical Review of Occupational Exposures and Cancer Risks in Medical Radiation Workers, *Radiation Research*, 174(6b), 793–808.
2. Mould, R. F. (1998). The discovery of radium in 1898 by Maria Sklodowska-Curie (1867-1934) and Pierre Curie (1859-1906) with commentary on their life and times. *The British Journal of Radiology*, 71(852), 1229–1254.
3. Stuewer, R. H. (1986). Rutherford's Satellite Model of the Nucleus. *Historical Studies in the Physical and Biological Sciences*, 16(2), 321–352.
4. Rana, M. A., & Qureshi, I. . (2002). Studies of CR-39 etch rates. *Nuclear Instruments and Methods in Physics Research Section B: Beam Interactions with Materials and Atoms*, 198(3-4), 129–134.
5. Misra, N. N., Yopez, X., Xu, L., & Keener, K. (2018). In-package cold plasma technologies. *Journal of Food Engineering*.
6. Zhu, Y., Li, C., Cui, H., & Lin, L. (2020). Feasibility of cold plasma for the control of biofilms in food industry. *Trends in Food Science & Technology*.
7. Perlman, I., Ghiorso, A., & Seaborg, G. T. (1950). Systematics of Alpha-Radioactivity. *Physical Review*, 77(1), 26–50.
8. Lang, P. F. (2021). Fermi energy, metals and the drift velocity of electrons. *Chemical Physics Letters*, 770, 138447.
9. Jönsson, G. (1995). Radon gas — where from and what to do? *Radiation Measurements*, 25(1-4), 537–546.
10. M.D. Salim, Nontraditional Methods for Different Types of Solid State Nuclear Track Detectors to Get Optimum Etching Parameters, Mustansiriyah University, Ph.D.thesis,(2020).
11. C.S. Oliveira, B. Malheiros, K.C.C. Pires , M. Assunção, S. Guedes, J.N. Corrêa, and S.A. Paschuk, Low energy alpha particle tracks in CR-39 nuclear track detectors: Chemical etching studies, *Nuclear Inst. and Methods in Physics Research*, A, 995 (2021) 165130.

12. G.S. Sahoo, S. Paul, S.P. Tripathy, S.C. Sharma, S. Jena, S. Rout, D.S. Joshi, and T. Bandyopadhyay, Effects of neutron irradiation on optical and chemical properties of CR-39: Potential application in neutron dosimetry, *Applied Radiation and Isotopes* 94 (2014) 200–205.
13. Ahmed A.I., and Wathab H.Y., Effect of Etching Solution on Nuclear Track Detector CR-39, *International Journal of Applied Engineering Research* ISSN 0973-4562 Volume 13, Number 10 (2018) pp. 8659-8663.
14. L. I. Kravets, V. M. Elinson, R. G. Ibragimov, B. Mitu, and G. Dinescu, Plasma surface modification of polypropylene track-etched membrane to improve its performance properties, *IOP Conf. Series: Journal of Physics: Conf. Series* 982 (2018) 012011.
15. Hamid H. Murbat, Nisreen Khaleel, Dawser H. Ghayb, and Fatima A. Khudair, Using non-thermal atmospheric argon plasma as a new technique in etching CR-39 nuclear track detector, Patent registered with the Central Agency for Standardization and Quality Control No. 4674 dated 8/24/2016.
16. Tripathy, S. P., Kolekar, R. V., Sunil, C., Sarkar, P. K., Dwivedi, K. K., & Sharma, D. N. (2010). Microwave-induced chemical etching (MCE): A fast etching technique for the solid polymeric track detectors (SPTD). *Nuclear Instruments and Methods in Physics Research Section A: Accelerators, Spectrometers, Detectors and Associated Equipment*, 612(2), 421–426.
17. Dwaikat, N., Iida, T., Sato, F., Kato, Y., Ishikawa, I., Kada, W., ... Ihara, Y. (2007). Study etching characteristics of a track detector CR-39 with ultraviolet laser irradiation. *Nuclear Instruments and Methods in Physics Research Section A: Accelerators, Spectrometers, Detectors and Associated Equipment*, 572(2), 826–830.
18. Vadym Prysiashnyi, *Journal of Surface Engineered Materials and Advanced Technology*, 2013, 3, 138-145.
19. T. Desmet, R. Morent, N. De Geyter, C. Leys, E. Schacht and P. Dubruel, *Biomacromolecules*, Vol. 10, No. 9, 2009, pp. 2351-2378.
20. R. Morent, N. De Geyter, J. Verschuren, K. De Clerck, P. Kiekens and C. Leys, *Surface & Coatings Technology*, Vol. 202, No. 14, 2008, pp. 3427-3449.
21. M. J. Shenton and G. C. Stevens, *Journal of Physics D: Applied Physics*, Vol. 34, No. 18, 2001, pp. 2761-2768.
22. T. Yamamoto, A. Yoshizaki, T. Kuroki and M. Okubo, *IEEE Transactions on Industrial Applications*, Vol. 40, No. 5, 2004, pp. 1220-1225.
23. Gleizes, A., Gonzalez, J. J., & Freton, P. (2005). Thermal plasma modelling. *Journal of Physics D: Applied Physics*, 38(9), R153–R183.

24. Thirumdas, R., Sarangapani, C., & Annapure, U. S. (2014). Cold Plasma: A novel Non-Thermal Technology for Food Processing. *Food Biophysics*, 10(1), 1–11.
25. Bernstein, I. B. (1958). Waves in a Plasma in a Magnetic Field. *Physical Review*, 109(1), 10–21.
26. Rochau, G. A., Bailey, J. E., Falcon, R. E., Loisel, G. P., Nagayama, T., Mancini, R. C., ... Liedahl, D. A. (2014). ZAPP: The Z Astrophysical Plasma Properties collaboration. *Physics of Plasmas*, 21(5), 056308.
27. Shukla, P. K. (2001). A survey of dusty plasma physics. *Physics of Plasmas*, 8(5), 1791–1803.
28. Dulk, G. A. (1985). Radio Emission from the Sun and Stars. *Annual Review of Astronomy and Astrophysics*, 23(1), 169–224.
29. Roth, J. R. (1995). Ball Lightning: What Nature is Trying to Tell the Plasma Research Community. *Fusion Technology*, 27(3), 255–270.
30. Sandholt, P. E., Deehr, C. S., Egeland, A., Lybekk, B., Viereck, R., & Romick, G. J. (1986). Signatures in the dayside aurora of plasma transfer from the magnetosheath. *Journal of Geophysical Research*, 91(A9), 10063.
31. Von Engel, A., & Cozens, J. R. (1965). Flame Plasmas. *Advances in Electronics and Electron Physics*, 99–146.
32. Grach, S. M., Sergeev, E. N., Mishin, E. V., & Shindin, A. V. (2016). Dynamic properties of ionospheric plasma turbulence driven by high-power high-frequency radiowaves. *Uspekhi Fizicheskikh Nauk*, 186(11), 1189–1228.
33. Kennel, C. F. (1969). Consequences of a magnetospheric plasma. *Reviews of Geophysics*, 7(1, 2), 379.
34. Rauscher, H., Perucca, M., & Buyle, G. (Eds.). (2010). *Plasma Technology for Hyperfunctional Surfaces*.
35. Moon, S. Y., Choe, W., & Kang, B. K. (2004). A uniform glow discharge plasma source at atmospheric pressure. *Applied Physics Letters*, 84(2), 188–190.
36. Forde, E., Guiney, I., Arshak, K., Adley, C., Barry, C., & Jordan, K. (2008). Theoretical and Experimental Considerations for Bacteria Sterilization Using a Novel Multielectrode Dielectric-Barrier Discharge System. *IEEE Transactions on Plasma Science*, 36(5), 2805–2815.
37. Chang, J.-S., Lawless, P. A., & Yamamoto, T. (1991). Corona discharge processes. *IEEE Transactions on Plasma Science*, 19(6), 1152–1166.

38. Laroussi, M., & Akan, T. (2007). Arc-Free Atmospheric Pressure Cold Plasma Jets: A Review. *Plasma Processes and Polymers*, 4(9), 777–788.
39. Chen, Z., Garcia, G., Arumugaswami, V., & Wirz, R. E. (2020). Cold atmospheric plasma for SARS-CoV-2 inactivation. *Physics of Fluids*, 32(11), 111702.
40. Ammann, A. A. (2007). Inductively coupled plasma mass spectrometry (ICP MS): a versatile tool. *Journal of Mass Spectrometry*, 42(4), 419–427.
41. Deng, X. L., Nikiforov, A. Y., Vanraes, P., & Leys, C. (2013). Direct current plasma jet at atmospheric pressure operating in nitrogen and air. *Journal of Applied Physics*, 113(2), 023305.
42. Park, J., Henins, I., Herrmann, H. W., Selwyn, G. S., & Hicks, R. F. (2001). Discharge phenomena of an atmospheric pressure radio-frequency capacitive plasma source. *Journal of Applied Physics*, 89(1), 20–28.
43. Passow, M. L., Brake, M. L., Lopez, P., McColl, W. B., & Repetti, T. E. (1991). Microwave resonant-cavity-produced air discharges. *IEEE Transactions on Plasma Science*, 19(2), 219–228.
44. Cheng, C., Peng, L., Lei, X., Li-Ye, Z., Ru-Juan, Z., & Wen-Rui, Z. (2006). Development of a new atmospheric pressure cold plasma jet generator and application in sterilization. *Chinese Physics*, 15(7), 1544–1548.
45. Gadri, R. B., Roth, J. R., Montie, T. C., Kelly-Wintenberg, K., Tsai, P. P.-Y., Helfritsch, D. J., ... Chen, Z. (2000). Sterilization and plasma processing of room temperature surfaces with a one atmosphere uniform glow discharge plasma (OAUGDP). *Surface and Coatings Technology*, 131(1-3), 528–541.
46. [46] Koinuma, H., Ohkubo, H., Hashimoto, T., Inomata, K., Shiraishi, T., Miyanaga, A., & Hayashi, S. (1992). Development and application of a microbeam plasma generator. *Applied Physics Letters*, 60(7), 816–817.
47. [47] Tudoran, C., Roşu, M., & Coroş, M. (2020). A concise overview on plasma treatment for application on textile and leather materials. *Plasma Processes and Polymers*, 17(8), 2000046.
48. Misra, N., Bhatt, S., Arefi-Khonsari, F., & Kumar, V. (2021). State of the art in nonthermal plasma processing for biomedical applications: Can it help fight viral pandemics like COVID-19? *Plasma Processes and Polymers*, 18(7), 2000215.
49. Hirsh, R. F. (1981). A Conflict of Principles: The Discovery of Argon and the Debate over Its Existence. *Ambix*, 28(3), 121–130.
50. Landsberg, H. E. (1953). The origin of the atmosphere. *Scientific American*, 189(2), 82-87.

51. Tusek, J. (2000). Experimental research of the effect of hydrogen in argon as a shielding gas in arc welding of high-alloy stainless steel. *International Journal of Hydrogen Energy*, 25(4), 369–376.
52. Yamauchi, T. (2003). Studies on the nuclear tracks in CR-39 plastics. *Radiation Measurements*, 36(1-6), 73–81.
53. Guo, S.-L., Chen, B.-L., & Durrani, S. A. (2020). Solid-state nuclear track detectors. *Handbook of Radioactivity Analysis*, 307–407.
54. Zhang, Y., Wang, H. W., Ma, Y. G., Liu, L. X., Cao, X. G., Fan, G. T., ... & Fang, D. Q. (2019). Energy calibration of a CR-39 nuclear-track detector irradiated by charged particles. *Nuclear Science and Techniques*, 30(6), 87.
55. Eissa, M. F. (2011). Study of the effect of post-irradiation with low linear energy transfer on optical and spectral response of CR-39 polymeric material.
56. Cassou, R. M., & Benton, E. V. (1978). Properties and applications of CR-39 polymeric nuclear track detector. *Nuclear Track Detection*, 2(3), 173–179.
57. Rana, M. A. (2018). CR-39 nuclear track detector: An experimental guide. *Nuclear Instruments and Methods in Physics Research Section A: Accelerators, Spectrometers, Detectors and Associated Equipment*.
58. García, M. J., Amgarou, K., Domingo, C., & Fernández, F. (2005). Neutron response study of two CR-39 personal dosimeters with air and Nylon converters. *Radiation measurements*, 40(2-6), 607-611.
59. Joshirao, P. M., Shin, J. W., Vyas, C. K., Kulkarni, A. D., Kim, H., Kim, T., ... & Manchanda, V. K. (2013). Development of optical monitor of alpha radiations based on CR-39. *Applied radiation and isotopes*, 81, 184-189.
60. Chavan, V., Kalsi, P. C., Hong, S. W., & Manchanda, V. K. (2020). A new chemical etchant for the development of alpha tracks in CR-39 solid state nuclear track detector. *Nuclear instruments and methods in physics research section B: Beam interactions with materials and atoms*, 462, 82-89.
61. Jönsson, G. (1995). Radon gas — where from and what to do? *Radiation Measurements*, 25(1-4), 537–546.
62. Underwood, E. A. (1945). Wilhelm Conrad Röntgen (1845–1923) and the Early Development of Radiology. *Proceedings of the Royal Society of Medicine*, 38(12), 697–706.
63. Jönsson, B.-A. (2021). Henri Becquerel’s discovery of radioactivity – 125 years later. *Physica Medica*, 87, 144–146.

64. Mc Laughlin, J. (2012). An historical overview of radon and its progeny: applications and health effects. *Radiation Protection Dosimetry*, 152(1-3), 2–8.
65. George, A. C., Paschoa, A. S., & Steinhäusler, F. (2008). World History Of Radon Research And Measurement From The Early 1900's To Today. *AIP Conference Proceedings*.
66. Radford, E. P., & Renard, K. G. S. C. (1984). Lung Cancer in Swedish Iron Miners Exposed to Low Doses of Radon Daughters. *New England Journal of Medicine*, 310(23), 1485–1494.
67. Temuujin, J., Surenjav, E., Ruescher, C., & Vahlbruch, J. A. N. (2018). Processing fly ash with a radioactivity (Critical Review). *Chemosphere*.
68. Bruno, R. C. (1983). Sources of Indoor Radon in Houses: A Review. *Journal of the Air Pollution Control Association*, 33(2), 105–109.
69. Cinti, D., Vaselli, O., Poncia, P. P., Brusca, L., Grassa, F., Procesi, M., & Tassi, F. (2019). Anomalous concentrations of arsenic, fluoride and radon in volcanic-sedimentary aquifers from central Italy: Quality indexes for management of the water resource. *Environmental Pollution*.
70. Papastefanou, C. (2008). Chapter 2 Radioactive aerosols. *Radioactive Aerosols*, 11–58.
71. Martin, R. B. (1991). Radon in the home. *Journal of Chemical Education*, 68(4), 275.
72. Lorenzo-González, M., Torres-Durán, M., Barbosa-Lorenzo, R., Provencio-Pulla, M., Barros-Dios, J. M., & Ruano-Ravina, A. (2019). Radon exposure: a major cause of lung cancer. *Expert Review of Respiratory Medicine*.
73. Geiger, C., & Barnes, K. B. (1994). Indoor radon hazard: a geographical assessment and case study. *Applied Geography*, 14(4), 350–371.
74. Ramadani, F. (2021). Early detection of Diabetes Mellitus in transition countries–Kosovo. A. STRAKOSHA, A. DEDEJ, F. NASTO, S. LAKO, L. BERDICA, N. THERESKA, 74.
75. Poortinga, W., Cox, P., & Pidgeon, N. F. (2008). The Perceived Health Risks of Indoor Radon Gas and Overhead Powerlines: A Comparative Multilevel Approach. *Risk Analysis*, 28(1), 235–248.
76. Lee, H. A., Lee, W. K., Lim, D., Park, S. H., Baik, S. J., Kong, K. A., ... Park, H. (2015). Risks of Lung Cancer due to Radon Exposure among the Regions of Korea. *Journal of Korean Medical Science*, 30(5), 542.

77. Lantz, P. M., Mendez, D., & Philbert, M. A. (2013). Radon, Smoking, and Lung Cancer: The Need to Refocus Radon Control Policy. *American Journal of Public Health*, 103(3), 443–447.
78. Jones, A. P. (1999). Indoor air quality and health. *Atmospheric Environment*, 33(28), 4535–4564.
79. Landrigan, P. J. (2001). Children's environmental health: lessons from the past and prospects for the future. *Pediatric Clinics of North America*, 48(5), 1319–1330.
80. Archer, V. E., Coons, T., Saccomanno, G., & Hong, D.-Y. (2004). LATENCY AND THE LUNG CANCER EPIDEMIC AMONG UNITED STATES URANIUM MINERS. *Health Physics*, 87(5), 480–489.
81. Tomasek, L., Swerdlow, A. J., Darby, S. C., Placek, V., & Kunz, E. (1994). Mortality in uranium miners in west Bohemia: a long-term cohort study. *Occupational and Environmental Medicine*, 51(5), 308–315.
82. Williams, A. G., Chambers, S. D., Conen, F., Reimann, S., Hill, M., Griffiths, A. D., & Crawford, J. (2016). Radon as a tracer of atmospheric influences on traffic-related air pollution in a small inland city. *Tellus B: Chemical and Physical Meteorology*, 68(1), 30967.
83. Jasaitis, D., Vasiliauskienė, V., Chadyšienė, R., & Pečiulienė, M. (2016). Surface Ozone Concentration and Its Relationship with UV Radiation, Meteorological Parameters and Radon on the Eastern Coast of the Baltic Sea. *Atmosphere*, 7(2), 27.
84. Nazaroff, W. W. (1992). Radon transport from soil to air. *Reviews of Geophysics*, 30(2), 137.
85. Smith, A. L. (1987). Radioactive-Scale Formation. *Journal of Petroleum Technology*, 39(06), 697–706.
86. Gray, P. R. (1993). NORM Contamination in the Petroleum Industry. *Journal of Petroleum Technology*, 45(01), 12–16.
87. Abdelouas, A. (2006). Uranium Mill Tailings: Geochemistry, Mineralogy, and Environmental Impact. *Elements*, 2(6), 335–341.
88. W. Dixon, D. (2001). Radon Exposures from the Use of Natural Gas in Buildings. *Radiation Protection Dosimetry*, 97(3), 259–264.
89. Sukanya, S., Noble, J., & Joseph, S. (2020). Factors controlling the distribution of radon (^{222}Rn) in groundwater of a tropical mountainous river basin in Southwest India. *Chemosphere*, 128096.

90. Barbier, E. (2002). Geothermal energy technology and current status: an overview. *Renewable and Sustainable Energy Reviews*, 6(1-2), 3–65.
91. Smyth, H. D. (1945). Atomic Energy for Military Purposes. *Reviews of Modern Physics*, 17(4), 351–471.
92. Piciu, D. (2017). Principles of Nuclear Medicine. *Nuclear Endocrinology*, 3–8.
93. Robertson, A., Allen, J., Laney, R., & Curnow, A. (2013). The Cellular and Molecular Carcinogenic Effects of Radon Exposure: A Review. *International Journal of Molecular Sciences*, 14(7), 14024–14063.
94. Sgouros, G. (2008). Alpha-particles for targeted therapy. *Advanced Drug Delivery Reviews*, 60(12), 1402–1406.
95. Qaim, S. M., Spahn, I., Scholten, B., & Neumaier, B. (2018). Corrigendum to: Uses of alpha particles, especially in nuclear reaction studies and medical radionuclide production. *Radiochimica Acta*, 106(10), 873–873.
96. May, T. C., & Woods, M. H. (1979). Alpha-particle-induced soft errors in dynamic memories. *IEEE Transactions on Electron Devices*, 26(1), 2–9.

RESUME

Mohammed Khairi Hussein HUSSEIN, completed his primary and secondary education in the same city. He graduated from Barwanah Preparatory School for Boys. He began his education at Kirkuk University, College of Education for Pure Sciences, Department of Physics in 2017 and graduated in 2021. He started his master's studies at Karabuk University in 2022. He completed the master's program he started at the Department of Physics in 2024 at Karabuk University, Institute of Science, Department of Physics.